THE PENNSYLVANIA STATE UNIVERSITY
SCHREYER HONORS COLLEGE

DEPARTMENT OF MECHANICAL ENGINEERING

Near-Field Electroluminescent Refrigeration Device for Simultaneous High Cooling Power and High Coefficient of Performance

CHUN SEN LIU
SPRING 2024

A thesis
submitted in partial fulfillment
of the requirements
for a baccalaureate degree
in Mechanical Engineering
with honors in Mechanical Engineering

Reviewed and approved* by the following:

Linxiao Zhu
Assistant Professor of Mechanical Engineering
Thesis Supervisor

Daniel Cortes
Associate Professor of Mechanical Engineering
Honors Adviser

* Electronic approvals are on file.

ABSTRACT

Over the past decades, there has been an extreme amount of development in the electronics industry. One challenge to further increasing the computational power is to cope with the excessive amount of heat generated in the computing process. To continue with increasing computational power and ensuring stability and safety of computing facilities, advanced cooling strategy is in high demand. Currently, the most common mode of heat transfer for electronics involve convection and conduction. On the other hand, for many emerging applications such as personalized thermal management, cooling of sensors, residential, industrial, and space cooling, efficient, solid-state cooler will be desirable.

The latest development in electroluminescent cooling involves using forward-biased light emitting diodes (LEDs) to achieve either high cooling power using near-field enhanced energy transfer or high coefficient of performance by using photon recycling in the far field. However, it is unclear if high cooling power and high coefficient of performance can be achieved in a same device. In this thesis, we theoretically demonstrate solid-state electroluminescent cooling with both high cooling power and high coefficient of performance. The total heat transfer between two parallel plates separated by a nanoscale or microscale gap is calculated. Both high cooling power and high coefficient of performance can be achieved using select films on the parallel plate structure with a supplied voltage. The performance of the cooling device is shown through a power-voltage relation. A setup with no film, and two with different films is tested. The device consisting of a GaAs LED and GaAs photodiode (PD) with a diamond film exhibits the highest cooling power and coefficient of performance since it enhances luminescent energy transfer, while suppressing sub-bandgap parasitic radiative heat transfer.

TABLE OF CONTENTS

LIST OF FIGURES

LIST OF TABLES

ACKNOWLEDGEMENTS

This thesis serves as a representation of all my work done in undergraduate research. I would like to thank everyone who has made an impact on my undergraduate education at Penn State. To begin, I am thankful for all the opportunities that Dr. Linxiao Zhu has given me in the past three years. Before I was a Schreyer Scholar, I worked in Dr. Zhu's lab out of personal interest. I had the opportunity of working on numerous projects before deciding on my current thesis topic. Dr. Zhu was always patient and willing to answer all my questions about radiative cooling. In the development of this thesis, Dr. Zhu took a lot of time out of his busy schedule to meet with me and provide guidance on computing data for this thesis.

I would also like to thank my honors advisor, Dr. Daniel Cortes. Dr. Cortes has given me much guidance on planning my Schreyer courses and thesis. Aside from of being a great professor in lecture, Dr. Cortes was always willing to talk about my concerns with graduate school and helping me develop the writing of my thesis.

Outside of my thesis committee, I would like to thank my friends and family. I have grown tremendously in my personal life as well as my academic pursuits. To say the last four years were challenging and eventful would be an understatement. All the great friends that I have made along the way has inspired me to push myself to be a great student, as well as giving me support throughout the low points of my career. As I continue my pursuit in academics, I want to be able to look back on this time and be grateful for everyone who I have met during these four years, and I hope this thesis summarizes my academic life as an undergraduate researcher.

Chapter 1

Introduction

1.1 Motivation

Radiative heat transfer relies on blackbody radiation of an object. The blackbody spectral intensity is governed by the Planck distribution [1]:

$$I_{\lambda,b}(\lambda, T) = \frac{2hc_o^2}{\lambda^5 \left[\exp\left(\frac{hc_o}{\lambda k_B T}\right) - 1\right]}. \quad (1)$$

The Planck distribution is a function of the wavelength of light λ in micrometers (μm) and the absolute temperature T of the emitting body in Kelvin (K). The Planck distribution contains natural constants where the Planck constant $h = 6.626 \times 10^{-34}\, J \cdot s$, the speed of light in a vacuum $c_0 = 2.998 \times 10^8\, m/s$, and the Boltzmann constant $k_B = 1.381 \times 10^{-23}\, J/K$. The total emissive power of a blackbody per unit area after accounting for radiation at all wavelengths and angles is $E = \sigma T^4$, where σ is the Stefan Boltzmann constant $\sigma = 5.67 \times 10^{-8}\, W/m^2K^4$. At a temperature of 300 K, this amounts to $460\, W/m^2$. The thermal radiation of a blackbody only depends on temperature. When the radiation emitted from one body is absorbed by another body, this leads to radiative heat transfer. For two flat semi-infinite blackbodies 1 and 2 at temperatures of T_1 and T_2 respectively, separated by a distance that is much bigger than the Wien's wavelength (~10 μm at 300 K) – also known as the far field regime, the net radiative heat transfer from body 1 to body 2 is $\sigma(T_1^4 - T_2^4)$. This is the maximum radiative heat transfer that can be exchanged

between two macroscopic bodies in the far field regime, which is also known as the blackbody limit. However, if the distance between the two bodies is smaller than the wavelength of light emitted by the two bodies, the blackbody limit can break down [2].

In 1964, a group from RCA Laboratories in Princeton performed a study showing that it was possible for a Gallium Arsenide (GaAs) diode to emit photons with energy higher than qV, which is the energy needed for injecting an electron-hole pair, where V is the voltage bias [3]. By showing that evidence, the study pointed to the possibility of electroluminescent cooling. The promise of electroluminescent cooling devices opens possibilities to solid state coolers. Unlike traditional refrigerators that require compressors, solid state coolers eliminate vibrations, and can be extremely compact and lightweight. However, the potential for the use of LEDs is limited by the efficiency of the wall-plug efficiency of LEDs. For the possibility of refrigeration, the wall-plug efficiency of an LED must exceed 100% [4], as hinted by Ref. [3]. In 1996, an experimental study achieved a quantum efficiency of 96% by lowering recombination velocities using GaInP. The study showed that index matching allows for a greater efficiency. However, the quantum efficiency does not exceed 100%, yielding no cooling [5]. In 2012, Santhanam et. al used an LED at low forward bias voltage. The experiment showed that at a low bias, the power of emitted optical light exceeds the input electrical power, indicating electroluminescent cooling [6]. In 2015, Chen et. al theoretically proposed a near-field electroluminescent cooling device to enhance the cooling performance via nanoscale enhancement [7].

1.2 Problem Statement

Currently, there are no theoretical or experimental results showing that a near-field electroluminescent cooling device can simultaneously achieve high cooling power and high coefficient of performance. This thesis aims to achieve this goal using photon recycling to enhance coefficient of performance and using near-field radiative heat transfer to enhance the power density. A powerful and efficient solid-state cooler would be able to provide a solution to advanced cooling strategies in various applications.

1.3 Organization of the Thesis

This thesis consists of six chapters that provides a background to near-field electroluminescent cooling and a review of current literature in the field (Chapter 2), the methodology behind the numerical experiment (Chapter 3), the results of the numerical experiment (Chapter 4), future improvements for a better near-field electroluminescent cooling setup (Chapter 5), and Conclusion (Chapter 6).

The governing equations of near-field radiative cooling and electroluminescent cooling are discussed in the background section in the second chapter. A literature review is performed to introduce the historical development of the concept of electroluminescent cooling. The background section highlights the important equations used in the computation process, while the methods section describes the variables that are used in the numerical experiment. The methods section will then be followed by the results section, where three geometries with different film materials are discussed. The cooling power, coefficient of performance, and mechanism for

enhanced performance are discussed. A chapter will be dedicated to the limitations of this work and future directions that can be explored.

Chapter 2

Background and Literature Review

2.1 Chemical Potential of Photons

Near-field electroluminescent cooling is an emerging field of research built on controlling electromagnetic energy transfer using the chemical potential of light and near-field radiative energy transfer. This chapter will discuss the governing equations of near-field radiative heat transfer, the workings principles of electroluminescent cooling, and near-field electroluminescent setups that have been attempted in the past.

For a semiconductor junction, at photon energy $\hbar\omega$ above the bandgap E_g, temperature T, and voltage bias V, the average photon energy for a mode, is governed by a Bose-Einstein distribution with chemical potential qV [7]:

$$\Theta(\omega, T, V) = \frac{\hbar\omega}{\exp\left(\frac{\hbar\omega - qV}{k_B T}\right) - 1}. \tag{2}$$

Here, ω is the angular frequency. The Bose-Einstein distribution of a semiconductor junction allows the photon emission to be tuned by voltage. Such tuning can enhance or suppress radiation by using a positive or negative voltage bias, respectively. The voltage will be a positive value that is below $E_g = \hbar\omega_c$. The chemical potential for photons in a semiconductor junction results from the dependence of electrons and holes on voltage bias, and dependence of radiative combination on the electron and hole concentration [8]. We note that for a body that does not have a semiconductor junction, the chemical potential for light is zero, and Eq. 2 is reduced to

$$\Theta(\omega, T) = \frac{\hbar\omega}{\exp\left(\frac{\hbar\omega}{k_B T}\right) - 1}. \tag{3}$$

2.2 Near-field Radiative Heat Transfer

Between two semi-infinite parallel plates 1 and 2 separated by a vacuum gap *d*, the net radiative heat transfer from plate 1 to plate 2 is given by:

$$q(T_1, T_2, d) = \int_0^\infty \frac{\Theta(\omega, T_1) - \Theta(\omega, T_2)}{4\pi^2} d\omega \int_0^\infty k\left[\tau_s(\omega, k) + \tau_p(\omega, k)\right] dk\,. \tag{4}$$

The absolute temperatures of the plates 1 and 2 are T_1 and T_2, respectively. Here, *k* denotes the parallel component of the wavevector. The τ_s and τ_p are the transmission probabilities for the transverse electric and transverse magnetic modes for the parallel plates, respectively, and they depend on the gap size [9]. The transmission probability functions have a closed-form analytical expression for semi-infinite plate-plate system. For radiative heat transfer between two multilayers or more complex geometries, either semi-analytical equations or numerical solvers must be used. The transmission probabilities are expressed with the following expression:

$$\tau_{\alpha=s,p}^{12}(\omega, k) = \begin{cases} \dfrac{(1 - |r_\alpha^{01}|^2)(1 - |r_\alpha^{02}|^2)}{|D_\alpha|^2}, & \text{if } k < \dfrac{\omega}{c}, \text{propagating waves} \\ \dfrac{4\mathrm{Im}(r_\alpha^{01})\mathrm{Im}(r_\alpha^{02})e^{-2\mathrm{Im}(\zeta_2)d}}{|D_\alpha|^2}, & \text{if } k > \dfrac{\omega}{c}, \text{evanascent waves} \end{cases}. \tag{5}$$

In Eq. 5, Fresnel reflection coefficients are represented by r_α^{ij}, and 0 represents the vacuum gap. For the transverse-electric polarization, $r_s^{ij} = (\zeta_i - \zeta_j)/(\zeta_i + \zeta_j)$, and for the transverse-magnetic polarization, $r_p^{ij} = (\epsilon_j\zeta_i - \epsilon_i\zeta_j)/(\epsilon_j\zeta_i + \epsilon_i\zeta_j)$, where $\zeta_i = \sqrt{\epsilon_i(\omega)\omega^2/c^2 - k^2}$ is the

perpendicular component of the wave vector and ϵ_i is the frequency dependent dielectric function, both in i-th layer. The term $\frac{1}{D_\alpha} = \frac{1}{1-r_\alpha^{01} r_\alpha^{02} e^{2i\zeta_2 d}}$ captures the interference effects due to multiple reflections between the two surfaces [9]. The heat transfer coefficient at a mean temperature T with small temperature differences is modeled as [9]:

$$h(T,d) \equiv \lim_{(T_1-T_2)\to 0} \left| \frac{q(T_1,T_2,d)}{T_1-T_2} \right| \equiv \int_0^\infty h_\omega(T,d)d\omega, \tag{6}$$

where $h_\omega(T,d) = \frac{1}{4\pi^2}\frac{\partial\Theta(\omega,T)}{\partial T}\int_0^\infty k\left[\tau_s(\omega,k)+\tau_p(\omega,k)\right]dk$. The heat transfer coefficient of different parallel plate materials plotted against the gap size is shown in Fig. 1 [9]. The photon transmission function depends on the permittivity, which is an optical property of a material. As the gap size falls below the wavelength of light, the heat transfer rate h for certain material systems can exceed the far-field limit by several orders of magnitude.

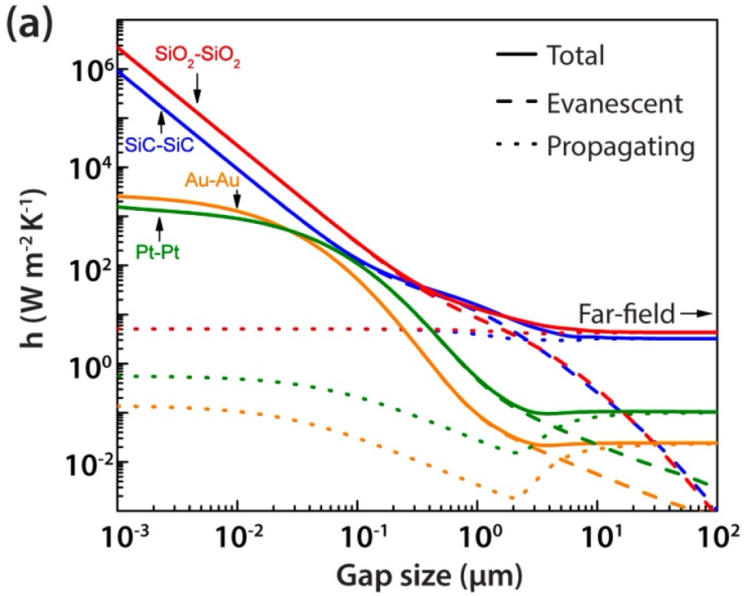

Figure 1. Heat transfer coefficient exceeds far-field limit by several magnitudes in the near-field regime [9]

2.3 Electroluminescent Cooling

Near-field enhanced electroluminescent cooling was theoretically proposed in 2015 by Chen et al. where a light emitting diode in close proximity to a receiver cools down to below the ambient temperature. To achieve this electroluminescent cooling, a positive bias V is applied onto the LED. The LED will then emit photons with energy that is slightly larger than the bandgap energy. When the applied voltage V is smaller than E_g/q, it is possible to achieve electroluminescent cooling. One may think that the mechanism violates the laws of thermodynamics. However, the difference in energy is extracted from the lattice vibrations within the semiconductor. Importantly, the emitted luminescence carried away non-zero entropy, making electroluminescent cooling thermodynamic possible. The electroluminescent cooling mechanism can be used to create a solid-state cooling device. Figure 2 shows an illustration of such solid-state cooling device.

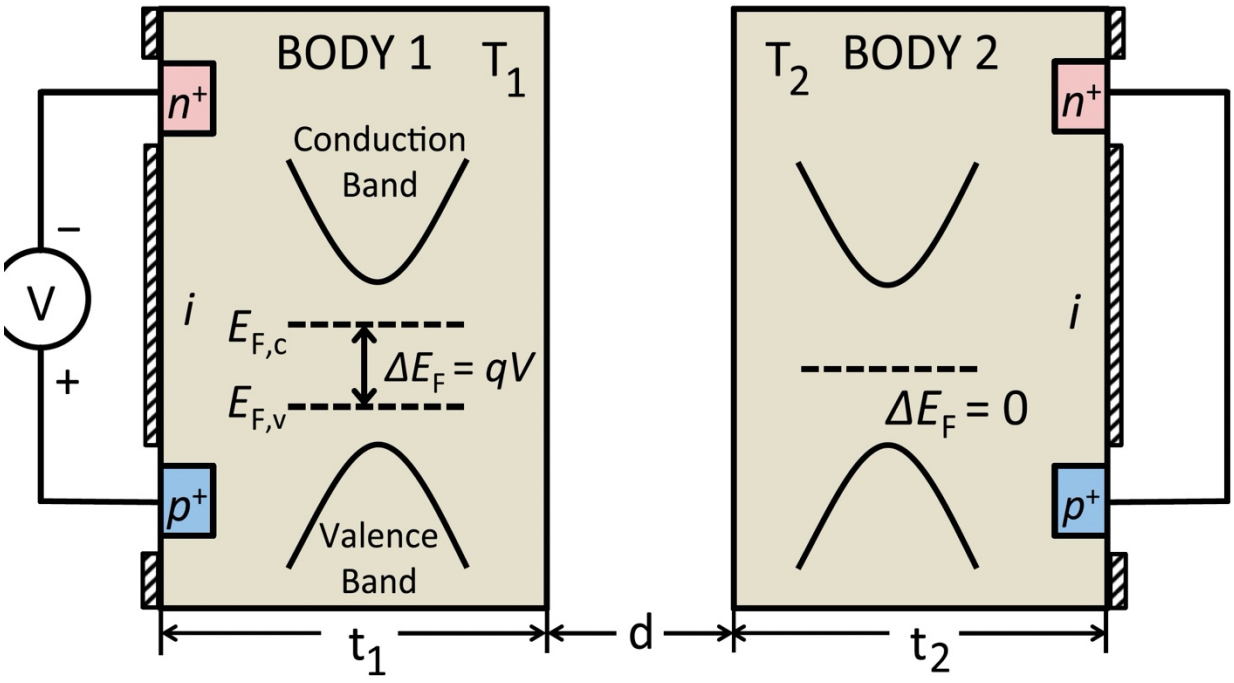

Figure 2. Example solid-state cooling device with voltage supplied to one side, reprinted with permission from [7]

For an electroluminescent cooler, the energy flux for above and below bandgap photons can be obtained using the following expressions:

$$E^{e}_{a\to b} = \int_{\omega_c}^{+\infty} \Theta(\omega, T_a, V_a)\Phi_e(\omega)d\omega \tag{7}$$

$$E^{p}_{a\to b} = \int_{0}^{\omega_c} \Theta(\omega, T_a, 0)\Phi_p(\omega)d\omega, \tag{8}$$

where the above bandgap portion is denoted using subscript *e*, while the below bandgap portion is denoted using subscript *p*. The $\Phi(\omega)$ term represents the photon transmission function that can be calculated numerically. Using a similar calculation, the above bandgap photon flux can also be calculated:

$$F_{a\to b} = \int_{\omega_c}^{+\infty} \frac{\Theta(\omega, T_a, V_a,)}{\hbar\omega} \Phi_e(\omega) d\omega. \tag{9}$$

Using reciprocity relation for photon transmission function and Eqs. 6-8, the net electromagnetic energy transfer from object 1 to object 2 at above bandgap range is [10]:

$$E^e = \int_{\omega_c}^{+\infty} [\Theta(\omega, T_1, V_1) - \Theta(\omega, T_2, V_2)] \Phi_e(\omega) d\omega, \tag{10}$$

the net electromagnetic energy transfer from body 2 to body 1 at below bandgap range is:

$$E^p = \int_{\omega_c}^{+\infty} [\Theta(\omega, T_2, 0) - \Theta(\omega, T_1, 0)] \Phi_p(\omega) d\omega, \tag{11}$$

and the net photon flux from object 1 to object 2 at above bandgap range is:

$$F = \int_{\omega_c}^{+\infty} \frac{\Theta(\omega, T_1, V_1)}{\hbar\omega} \Phi_e(\omega) d\omega - \int_{\omega_c}^{+\infty} \frac{\Theta(\omega, T_2, V_2)}{\hbar\omega} \Phi_e(\omega) d\omega. \tag{12}$$

To evaluate the energy balance of the LED, aside from electromagnetic energy transfer as discussed above, one also needs to account for the electrical work input to the LED which equals IV. The net cooling power density of the LED can be expressed as

$$Q_c = (E^e - E^p) - I_1 V_1, \tag{13}$$

where I_1 is the current density in the LED, i.e., object 1. Here, $E^e - E^p$ describes the net heat flow from body 1 to body 2. The currents in body 1 or body 2, due to the electromagnetic energy transfer between body 1 and body 2 at above bandgap photon energies are

$$I_1 = q(F + R_1) \tag{14}$$

$$I_2 = q(-F + R_2), \tag{15}$$

where the electron charge $q = 1.602176565 * 10^{-19}$ C. The total nonradiative recombination rate per unit area R_a can be calculated by accounting for the Auger recombination and the Shockley-Read-Hall (SRH) recombination:

$$R_a = \left(C_{n,a}n_a + C_{p,a}p_a\right)\left(n_a p_a - n_{i,a}^2\right)t_a + A_a \frac{n_a p_a - n_{i,a}^2}{n_a + p_a + 2n_{i,a}} t_a. \tag{16}$$

$C_{n,a}$ and $C_{p,a}$ are the Auger recombination coefficients for two-electron and two-hole processes of body a, respectively. n_a and p_a are electrons and holes density of body a, respectively. The intrinsic carrier concentration for body a is presented by $n_{i,a}$, and thickness of body a is t_a. A_a is the Shockley-Read-Hall recombination coefficient of body a that is dependent on the SRH lifetime $\tau_{SRH,a}$, where $A_a = 1/\tau_{SRH,a}$. The coefficient of performance can then be calculated using the following expression by accounting for the net electricity input to the system:

$$COP = \frac{Q_c}{I_1 V_1 + I_2 V_2} \tag{17}$$

2.4 Literature Review

In 2018, Xiao et al. proposed a design of electroluminescent cooler with high coefficient of performance which consists of a forward-biased LED facing a photovoltaic cell [11]. Both sides

are made of Gallium Arsenide (GaAs). The cold side is a GaAs LED, while the hot side is a GaAs photodiode (PD). The two plates are separated by a vacuum gap as seen in Fig. 3, where the light emitted by the LED will act as a working fluid that carries energy. In this application, the light emitted can act as a refrigerant for the system.

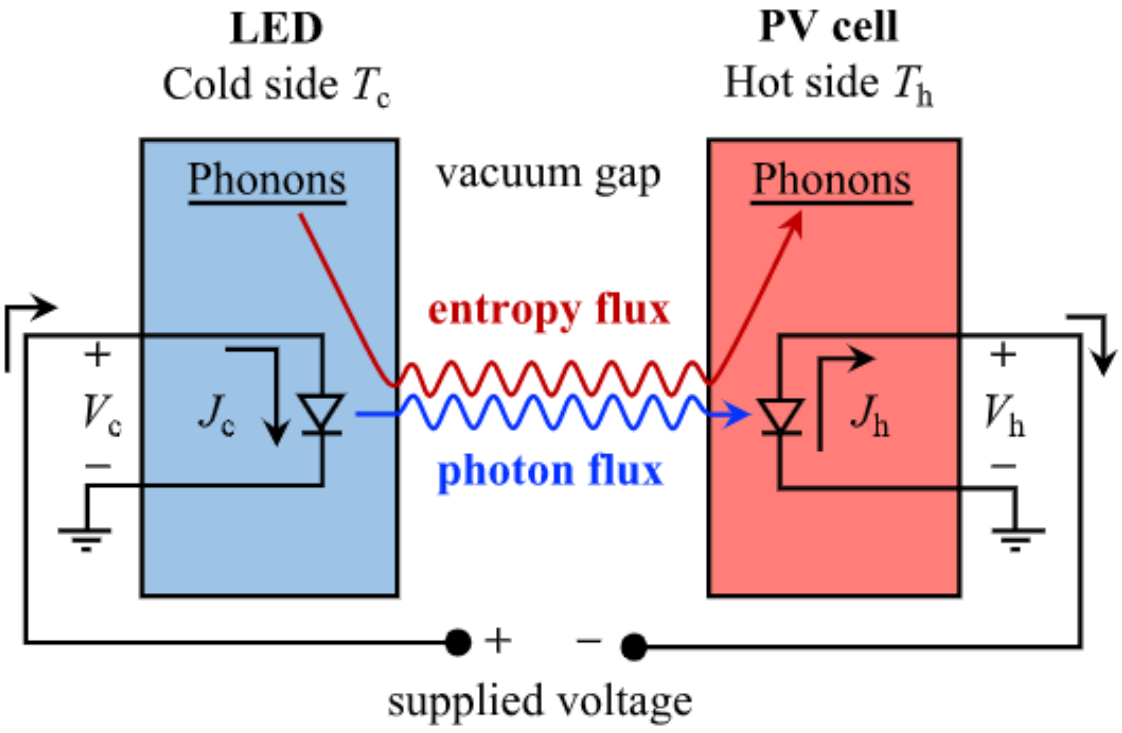

Figure 3. Schematic of electroluminescent refrigerator [11]

The hot photodiode will provide energy recovery by harvesting the light from the LED. Figure 4 [11] shows the cooling heat flux with respect to the voltage bias. The temperatures of the two sides are supposed to emulate a room temperature application. Figure 4 [11] shows a small difference in cooling heat flux between systems with PV recovery and without PV recovery. The reason why the heat flux is lower with PV recovery is because the PV cell will emit photons back to the LED. However, the coefficient of performance drastically increases with PV recovery, while sacrificing little cooling power as shown in Fig. 5 [11]. Note that the highest coefficient of performance and

the highest cooling flux are not achieved at the same operating point. Though the COP can approach 25% of the Carnot COP, the net cooling power density below 1000 W/m^2 is relatively small.

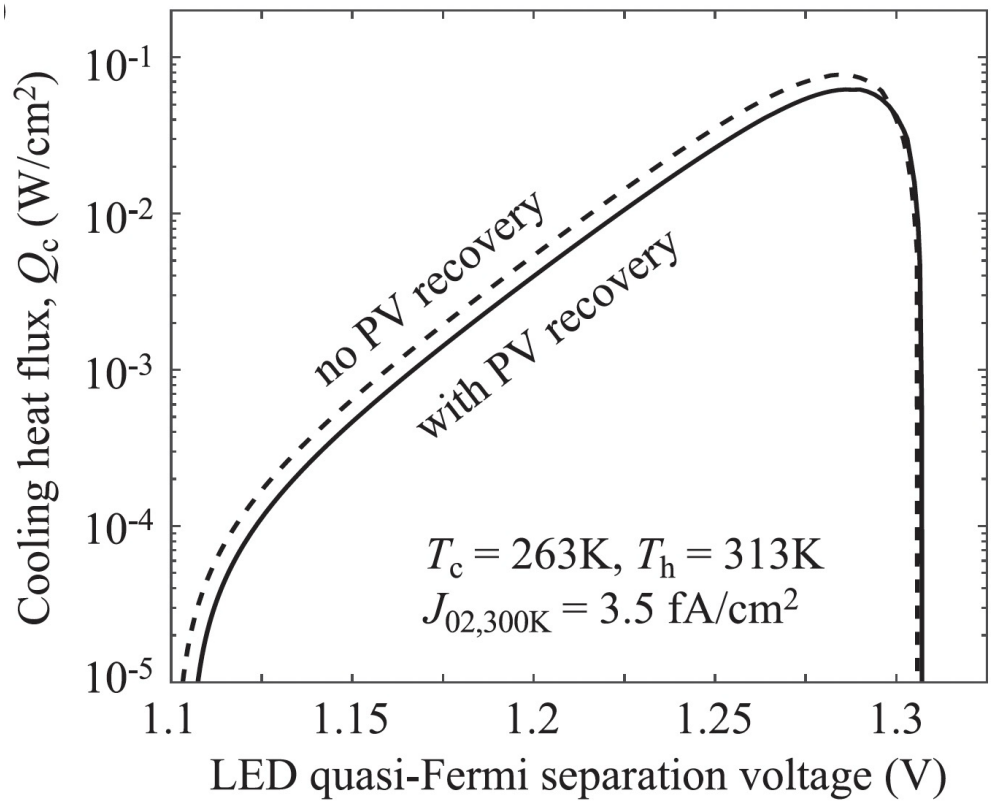

Figure 4. Cooling heat flux of two plate parallel systems with and without PV recovery [11]

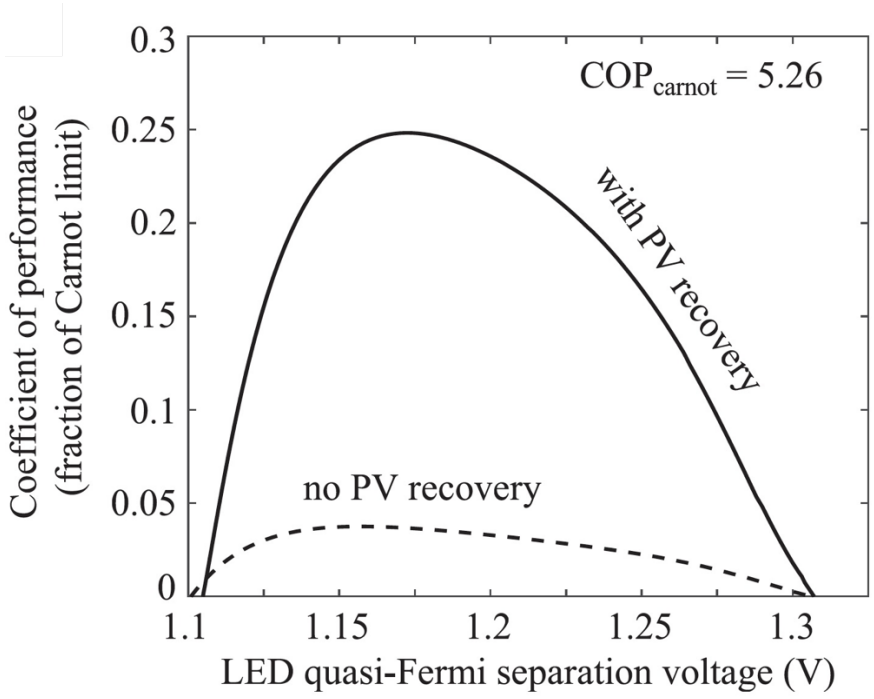

Figure 5. Coefficient of performance of two plate parallel systems with and without PV recovery [11]

Another study aimed at increasing the cooling power density by using near field radiative heat transfer. A GaAs LED is on the cold side. However, a Silicon (Si) PV cell is used for the hot side as shown in Fig. 6 [10].

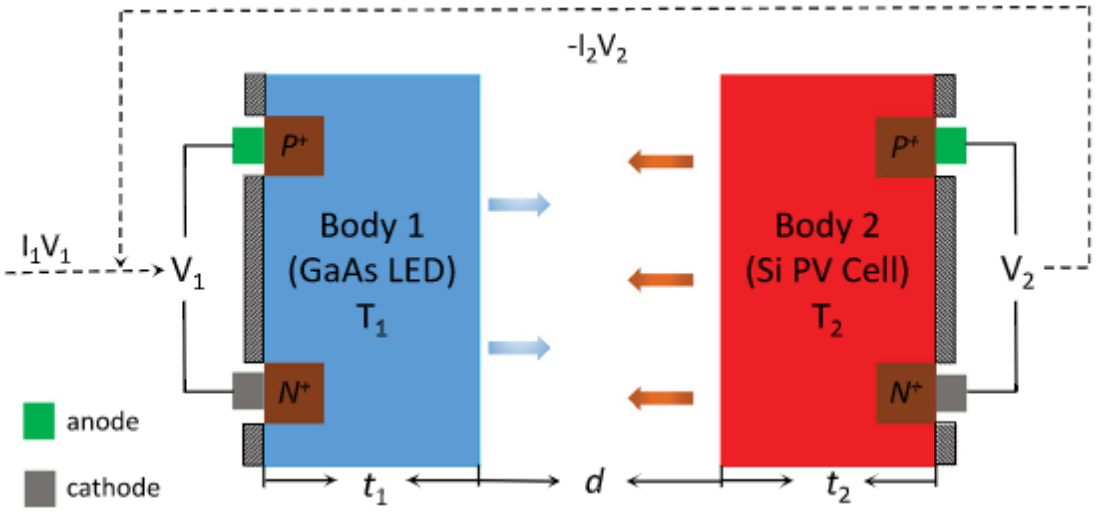

Figure 6. Schematic of electroluminescent refrigerator by Chen et al. reprinted with permission from [10]

The performance of the setup was assessed with and without PV power recovery. Fig. 7 shows the heat flux, and Fig. 8 shows the coefficient of performance of Chen's setup. The two curves denote two different distances between the two plates. In each curve, it can be compared to Ref. [11]. When the distance is 10nm, the cooling heat flux is far more significant than in Ref. [11]. In the near field, the cooling flux can reach 100 W/cm^2, while it is below 0.1 W/cm^2 as seen in Fig. 4 [11].

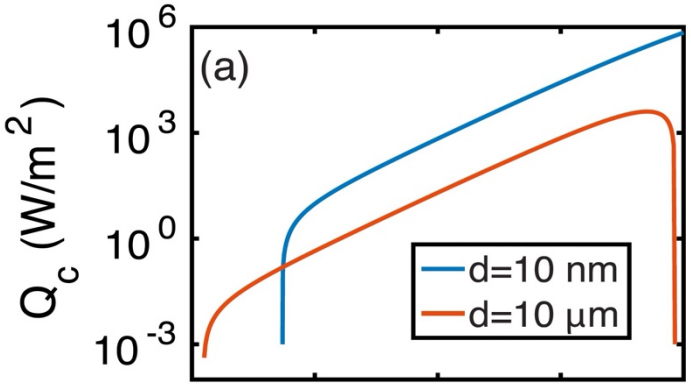

Figure 7. Heat flux of setup between two vacuum gaps without power recovery. Fig. 8 contains horizontal axis, reprinted with permission from [10]

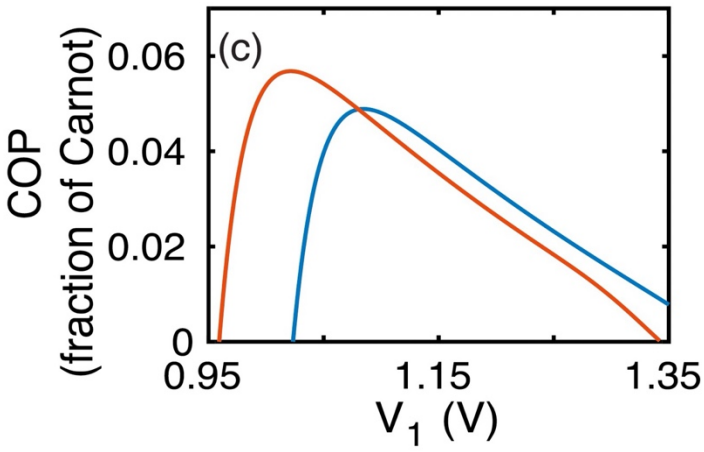

Figure 8. Coefficient of performance of setup between two band gaps without power recovery, reprinted with permission from [10]

The same configuration was also tested with power recovery. For each value of V_1 and gap size in the setup, there is an optimal voltage V_2 that is supplied to the PV cell. However, even with the optimal V_2, Fig. 9 shows that the COP is still relatively small, about 10% of the Carnot COP [10].

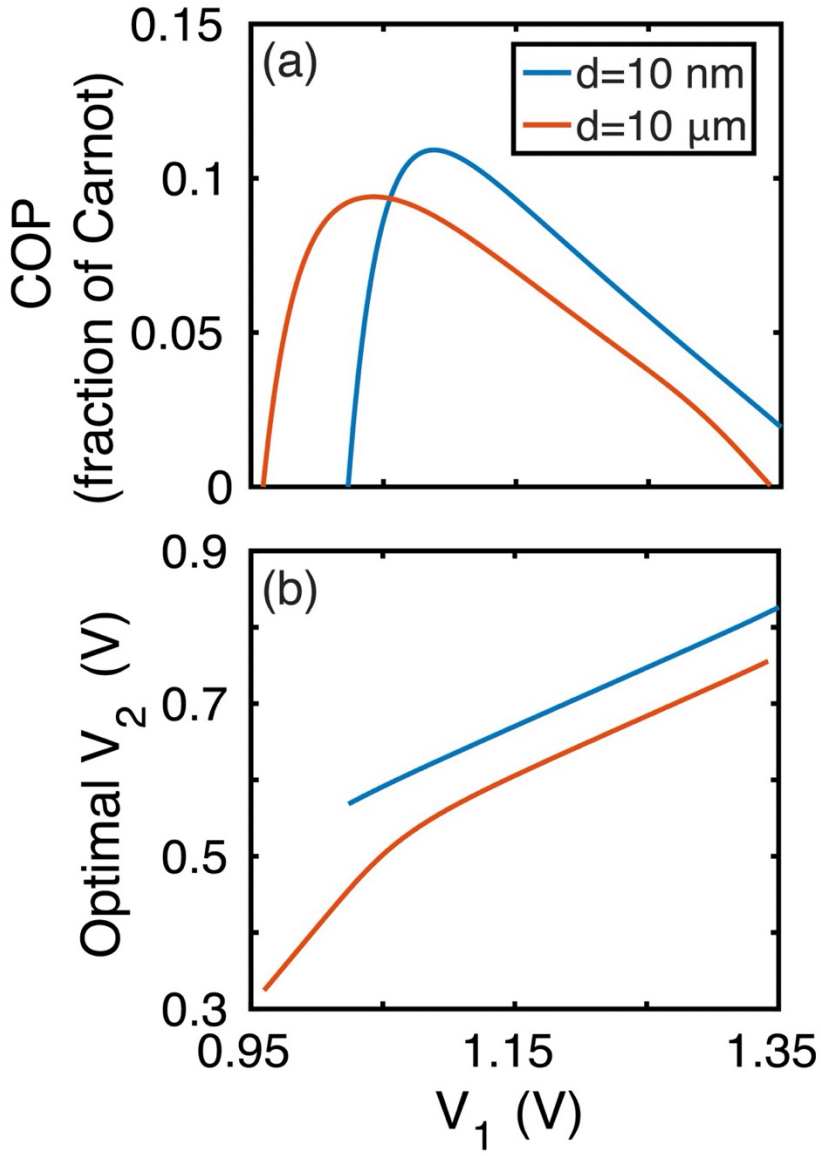

Figure 9. Coefficient of performance of setup between two band gaps with optimal power recovery, reprinted with permission from [10]

2.5 This work

This thesis aims to bridge the gap between high cooling flux and high coefficient of performance. Different materials drastically change the outcome of cooling flux and coefficient of performance. My work will focus on identifying a design that can provide a high cooling flux, while simultaneously increasing the coefficient of performance. Techniques in section 2.2 will be used to identify possible materials that can be used in this setup, following a design optimization process. Section 2.3 reviewed two studies that were aiming for different goals, one aiming for high cooling flux, one aiming for high efficiency. Currently, there is no theoretical design that can achieve over 0.1 W/cm^2 cooling power while with coefficient of performance above 15% of the Carnot COP.

Chapter 3

Methods

3.1 Design of the Numerical Experiment

This thesis aims to achieve both high cooling power and high coefficient of performance through computational methods. To enhance the cooling power, we will consider a nanoscale distance between the LED and the receiver, so that the energy transfer can be enhanced due to near-field tunneling. To achieve high coefficient of performance, we will use a photovoltaic cell to recycle the luminescence from the LED, and use a high-index infrared transparent material to suppress below-bandgap radiative heat transfer. To investigate the impact of the high-index infrared transparent layer, we considered three scenarios: a first receiver without such layer, a second receiver with a Si layer on top, a third receiver with a diamond layer on top.

3.2 Variables

The geometry of the three models remains constant throughout. The LED and photodiode (PD) will be denoted using subscript 1 and 2, respectively. Figure 10 shows an illustration of the geometry. A semi-infinite perfect electric conductor (PEC) is considered as the substrates for the LED and PD. The thickness of the GaAs LED and PD $t_{\mathrm{LED,PD}}$ are set to 0.5 μm, while the thickness of the film t_{film} is set to 0.25 μm. In the case of the model with no film, the film was set to a

thickness of 0. We perform modeling of two gap sizes including 10 μm and 10 nm. The gap is defined as the distance between the GaAs LED and the film.

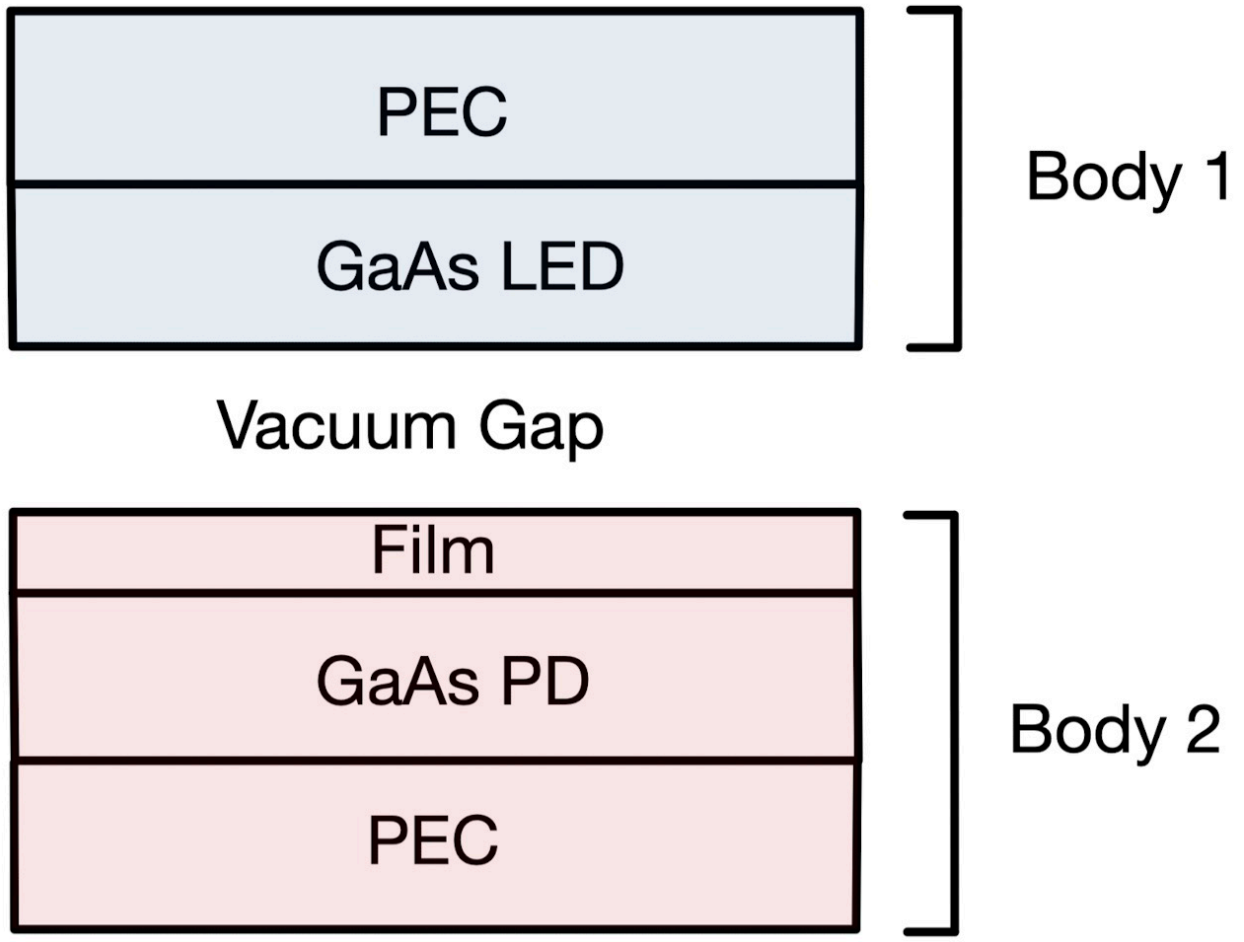

Figure 10. Geometry of the numerical experiment, cold side and hot side labeled with blue and red, respectively.

The temperature of the LED T_1 is set to 320 K, while the temperature of the PD T_2 is set to 330 K. The voltage to the LED V_1 will be varied from 1 V to 1.375 V. For each V_1, six different voltages for V_2 will be tested to assess the optimal voltage for the PD.

Table 1. List of Variables

No.	*Film*	*V_1 (V)*	*V_2 (V)*	*T_1 (K)*	*T_2 (K)*	*Gap (μm)*
1	None	1, 1.00375, …, 1.375	1.03750	320	330	0.01, 10

2	None	1, 1.00375, …, 1.375	1.18750	320	330	0.01, 10
3	None	1, 1.00375, …, 1.375	1.28125	320	330	0.01, 10
4	None	1, 1.00375, …, 1.375	1.30000	320	330	0.01, 10
5	None	1, 1.00375, …, 1.375	1.33750	320	330	0.01, 10
6	Silicon	1, 1.00375, …, 1.375	1.03750	320	330	0.01, 10
7	Silicon	1, 1.00375, …, 1.375	1.18750	320	330	0.01, 10
8	Silicon	1, 1.00375, …, 1.375	1.28125	320	330	0.01, 10
9	Silicon	1, 1.00375, …, 1.375	1.30000	320	330	0.01, 10
10	Silicon	1, 1.00375, …, 1.375	1.33750	320	330	0.01, 10
11	Diamond	1, 1.00375, …, 1.375	1.03750	320	330	0.01, 10
12	Diamond	1, 1.00375, …, 1.375	1.18750	320	330	0.01, 10
13	Diamond	1, 1.00375, …, 1.375	1.28125	320	330	0.01, 10
14	Diamond	1, 1.00375, …, 1.375	1.30000	320	330	0.01, 10
15	Diamond	1, 1.00375, …, 1.375	1.33750	320	330	0.01, 10

3.3 Calculation

All the calculations were performed on MATLAB and part of the code can be found in the appendix. A custom code of the Zhu Group calcEmit.m is used to calculate the photon transmission function between each pair of layers, and is dependent on the permittivity and thickness of each layer. The photon transmission function is represented with the following expression:

$$\Phi = \Phi(t_{gap}, t_{LED}, t_{film}, t_{PD}, T_1, T_2, V_1, V_2)$$

where every combination of the function from Table 1 in both above and below bandgap is calculated. Each study should have 202 Φ values. The total number of Φ values can be calculated as follows:

$$N_{\Phi} = length(V_1) * length(V_2) * length(Gap) * length(T_1)$$

Once the calculations for the Φ values are complete, Eqs. 7-17 can now be used. The Auger recombination coefficient for GaAs is $C_1 = 7 * 10^{-30} cm^6 s^{-1}$, while $C_{n,1}$ and $C_{p,1}$ both equal to $C_1/2$. Since both the LED and PD are GaAs, $C_1 = C_2$. The intrinsic carrier density $n_{i,1} = 2.8 * 10^5 cm^{-3}$ for GaAs. For GaAs, the time SRH lifetime $\tau_{SRH} = 16.7 * 10^{-6}\ \mu s$ [10]. Once all the variables are obtained, the total cooling power and coefficient of performance is calculated and plotted.

Chapter 4

Results & Analysis

All computations are performed in MATLAB. The computation time is dominated by the evaluation of Φ. Once all the net cooling flux Q_c and COP calculations were completed, all results were plotted on the same log scale against the voltage supplied to the LED V_1. Two gap sizes are tested and temperatures of the LED and PD are kept constant. The voltage supplied to the LED V_1 ranges from 1 V to 1.375 V, with step sizes of 0.00375 V.

4.1 Results of Study With No Film

We first study a case when the GaAs LED faces a GaAs PD without coating. The net cooling power and the optimized COP are shown in Figs. 11-15. Each figure in Figs. 11-15 corresponds to a different V_2. In each figure, the blue curve denotes $0.01\ \mu m$ gap case, which is in the near field regime, and the red curve denotes $10\ \mu m$ gap case, which is in the far field regime. As V_2 increases, the minimal V_1 needed to have net cooling increases. The magnitude of cooling in the near-field is magnitudes higher than the far-field, which follows the trend in Fig. 1. However, the coefficient of performance in the near-field is significantly lower than the far-field. The low coefficient of performance in the near-field results from the near-field enhanced sub-bandgap radiative heat transfer, which contributes as parasitic heating on the LED.

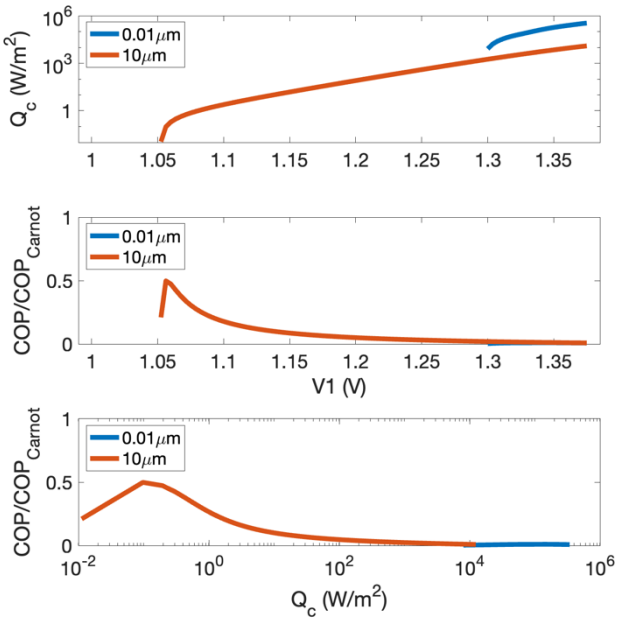

Figure 11. Cooling power and COP of GaAs LED and GaAs PD, without coating on PD. The temperatures of the LED and PD are 320 K and 330K, respectively, and the voltage bias of the PD is 1.0375 V

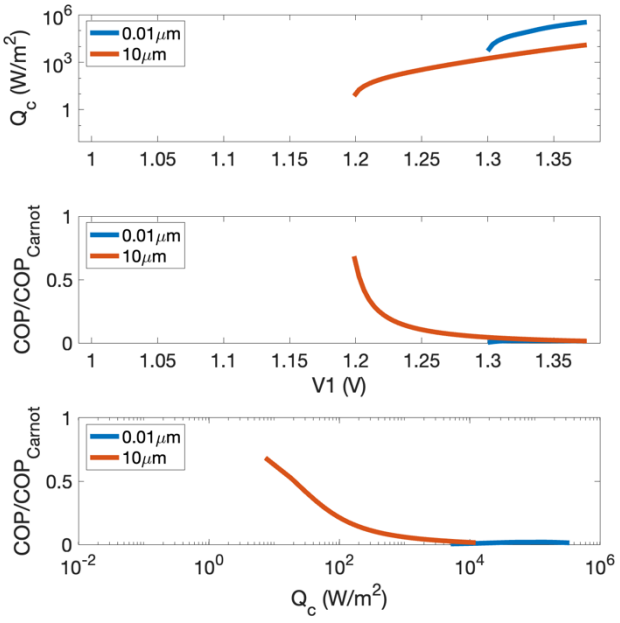

Figure 12. Cooling power and COP of GaAs LED and GaAs PD, without coating on PD. The temperatures of the LED and PD are 320 K and 330K, respectively, and the voltage bias of the PD is 1.1875 V

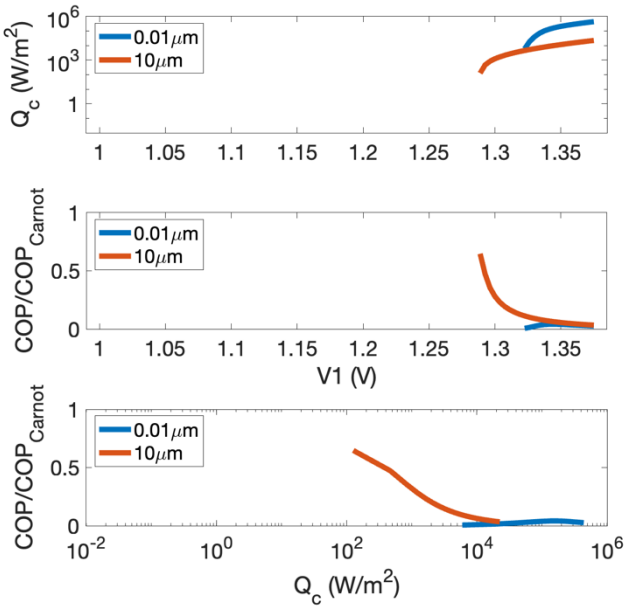

Figure 13. Cooling power and COP of GaAs LED and GaAs PD, without coating on PD. The temperatures of the LED and PD are 320 K and 330K, respectively, and the voltage bias of the PD is 1.2812 V

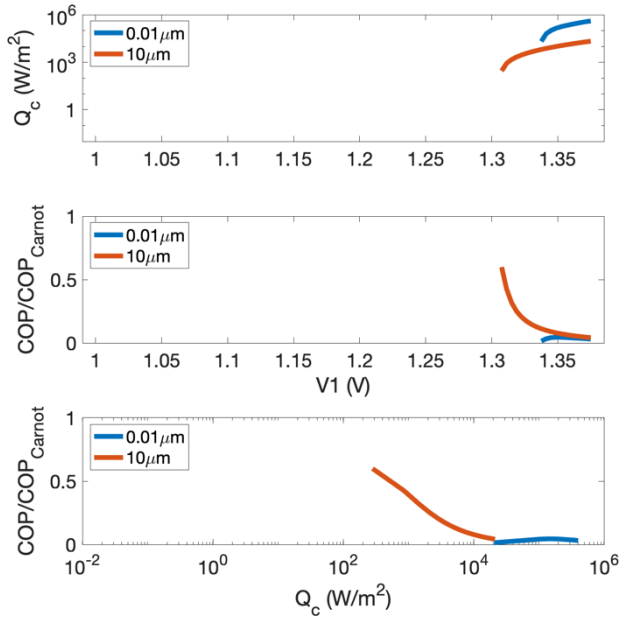

Figure 14. Cooling power and COP of GaAs LED and GaAs PD, without coating on PD. The temperatures of the LED and PD are 320 K and 330K, respectively, and the voltage bias of the PD is 1.3000 V

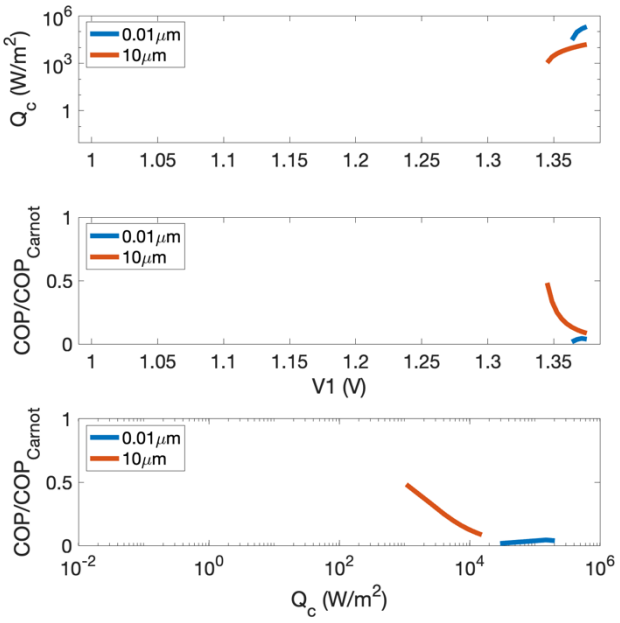

Figure 15. Cooling power and COP of GaAs LED and GaAs PD, without coating on PD. The temperatures of the LED and PD are 320 K and 330K, respectively, and the voltage bias of the PD is 1.3375 V

4.2 Results of study with Si film

To suppress the sub-bandgap parasitic heat transfer while maintaining the high cooling power, we add high-index infrared transparent layer on the PD. We first use Si as the coating. Si is chosen as Si has high refractive index and has little optical loss in the infrared wavelengths. The results for 5 different V_2 cases are shown in Figs. 16-20. The magnitude of cooling power remains largely unchanged. Unlike the curves from the studies without a film, there is now net cooling for a larger range of V_1 in the near-field scenario. The coefficient of performance in the near field is now similar to that in the far field. However, the Si film does not meet the goal of simultaneously achieving high cooling power and high coefficient of performance, as the coefficient of performance is still small. The undesirable feature with Si coating is that Si has a lower bandgap

than GaAs. Accordingly, Si can absorb the electroluminescence of GaAs LED, which otherwise can be recycled for electricity using GaAs PD. Thus, it will be beneficial to search for coating that has higher bandgap than GaAs, while being lossless in infrared wavelengths.

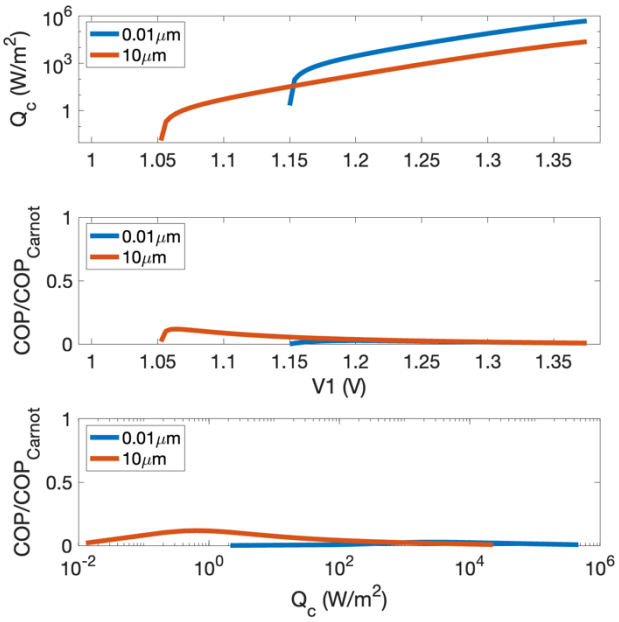

Figure 16. Cooling power and COP of GaAs LED and GaAs PD, with Si coating on PD. The temperatures of the LED and PD are 320 K and 330K, respectively, and the voltage bias of the PD is 1.0375 V

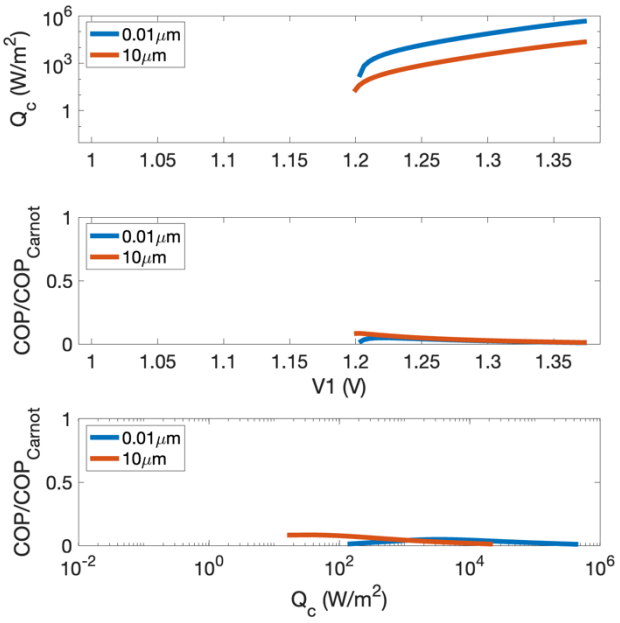

Figure 17. Cooling power and COP of GaAs LED and GaAs PD, with Si coating on PD. The temperatures of the LED and PD are 320 K and 330K, respectively, and the voltage bias of the PD is 1.1875 V

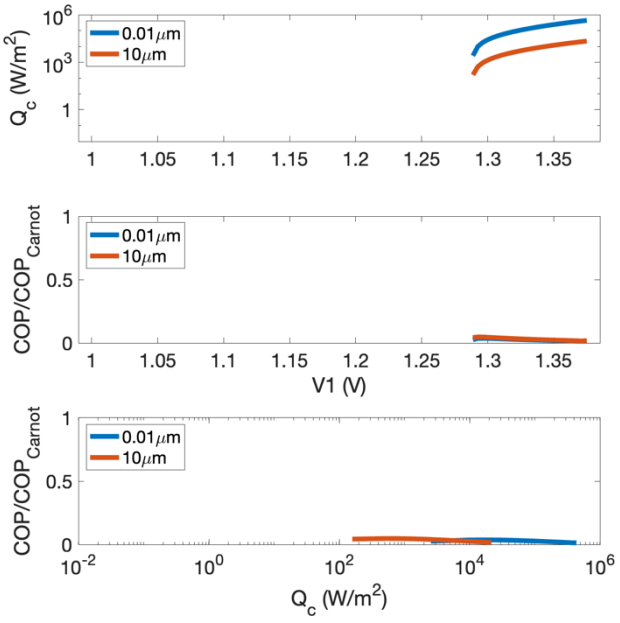

Figure 18. Cooling power and COP of GaAs LED and GaAs PD, with Si coating on PD. The temperatures of the LED and PD are 320 K and 330K, respectively, and the voltage bias of the PD is 1.2812 V

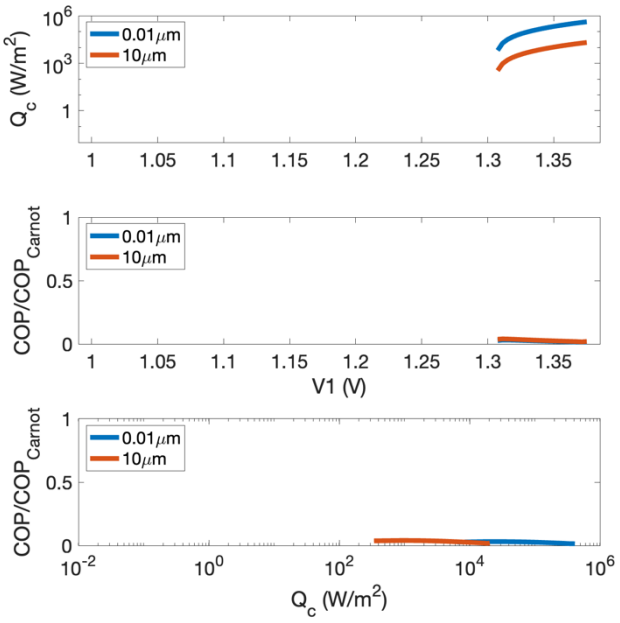

Figure 19. Cooling power and COP of GaAs LED and GaAs PD, with Si coating on PD. The temperatures of the LED and PD are 320 K and 330K, respectively, and the voltage bias of the PD is 1.3000 V

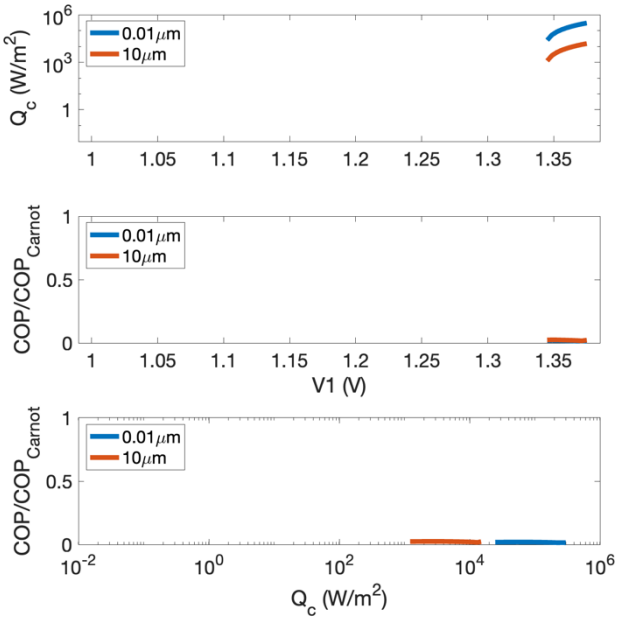

Figure 20. Cooling power and COP of GaAs LED and GaAs PD, with Si coating on PD. The temperatures of the LED and PD are 320 K and 330K, respectively, and the voltage bias of the PD is 1.3375 V

4.3 Results of study with Diamond film

We now consider diamond as the coating material. Diamond has high bandgap (5.47 eV) and is transparent all the way from ultraviolet to far infrared. Thus, diamond could serve as a good candidate for enhancing cooling performance. Figures 21-25 shows the studied performed with a diamond film. The magnitude of the cooling power remains unchanged. The diamond film also exhibits the same characteristics as the Si film, where the near-field regime has a larger V_1 range for achieving net cooling. However, the coefficient of performance of diamond case can greatly exceed the two previous cases. The studies with the diamond film is able to simultaneously achieve high cooling power and high coefficient of performance. For example at $V_2 = 1.3375\,V$, the cooling power can exceed 1 W/cm^2, and the COP exceeds 30% of the Carnot COP.

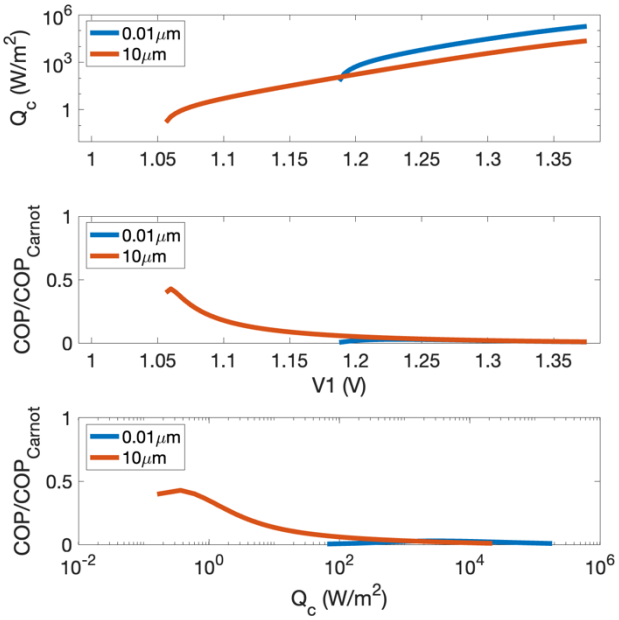

Figure 21. Cooling power and COP of GaAs LED and GaAs PD, with diamond coating on PD. The temperatures of the LED and PD are 320 K and 330K, respectively, and the voltage bias of the PD is 1.0375 V

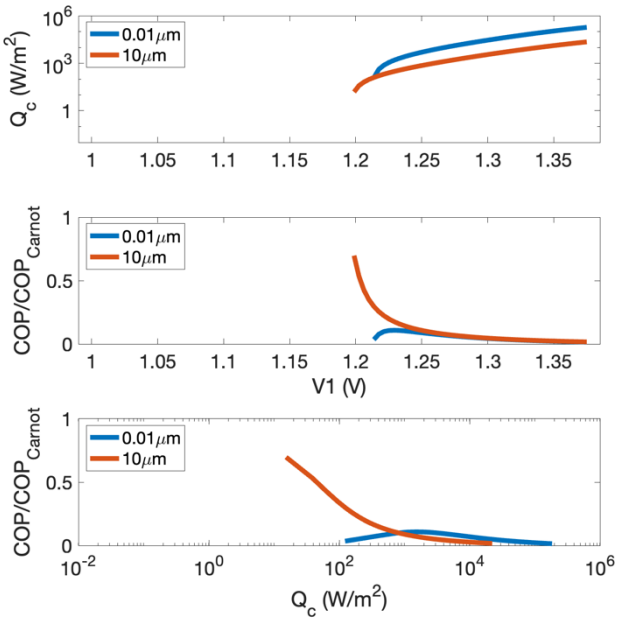

Figure 22. Cooling power and COP of GaAs LED and GaAs PD, with diamond coating on PD. The temperatures of the LED and PD are 320 K and 330K, respectively, and the voltage bias of the PD is 1.1875 V

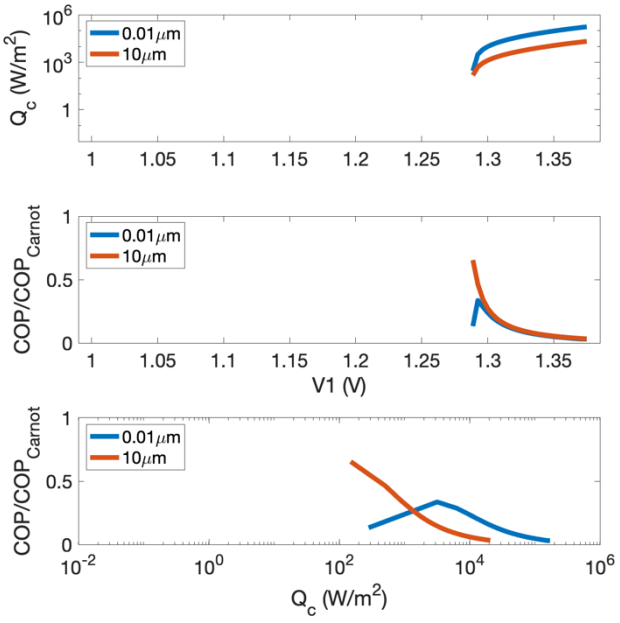

Figure 23. Cooling power and COP of GaAs LED and GaAs PD, with diamond coating on PD. The temperatures of the LED and PD are 320 K and 330K, respectively, and the voltage bias of the PD is 1.2812 V

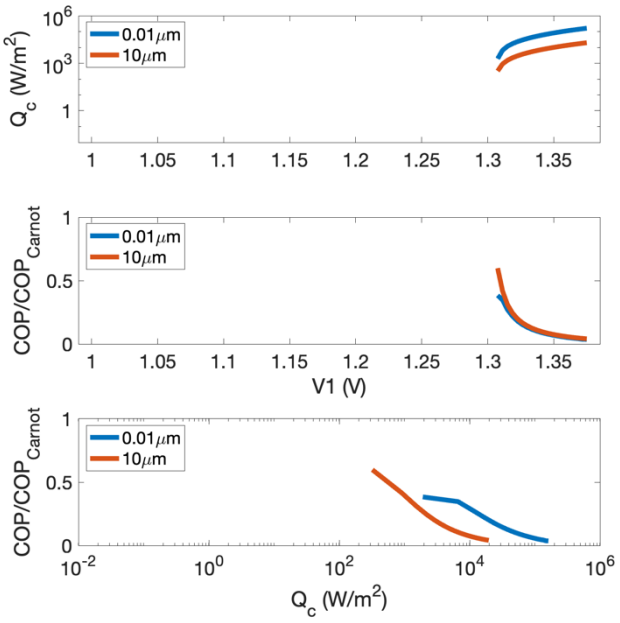

Figure 24. Cooling power and COP of GaAs LED and GaAs PD, with diamond coating on PD. The temperatures of the LED and PD are 320 K and 330K, respectively, and the voltage bias of the PD is 1.3000 V

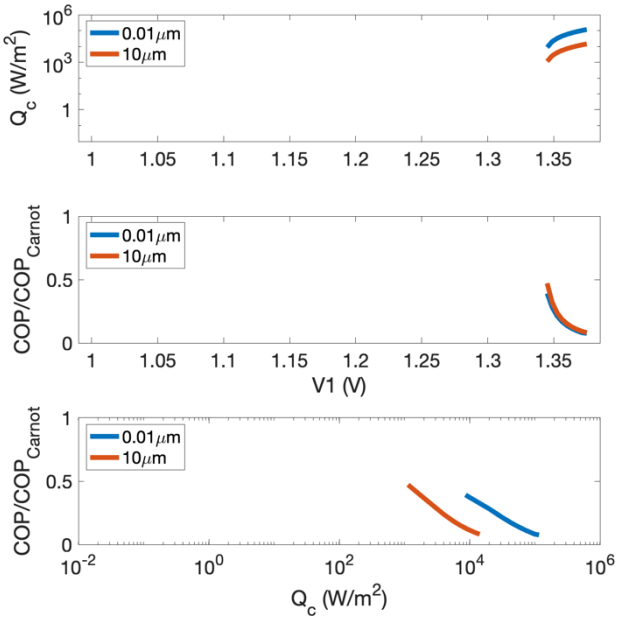

Figure 25. Cooling power and COP of GaAs LED and GaAs PD, with diamond coating on PD. The temperatures of the LED and PD are 320 K and 330K, respectively, and the voltage bias of the PD is 1.3375 V

4.4 Discussion and comparison of studies

All cases performed showed a maximum cooling flux at around $10^5 W/m^2$ for 10 nm gap case, however each study showed different a different coefficient of performance curve. Using different materials yielded different normalized photon transmission functions $\Phi/(\frac{1}{\lambda^2})$ for each configuration. Fig. 26 shows that in the far field, where the gap size is set to $10\mu m$, the application of films have little effect in changing the magnitude of $\Phi/(\frac{1}{\lambda^2})$. On the other hand, in the near field, $\Phi/(\frac{1}{\lambda^2})$ at below bandgap frequencies is decreased by several magnitudes when a film is present as shown in Fig. 27. Diamond and Si films are able to reduce sub-bandgap parasitic heating by limiting the sub-bandgap $\Phi/(\frac{1}{\lambda^2})$, which enhances the cooling performance.

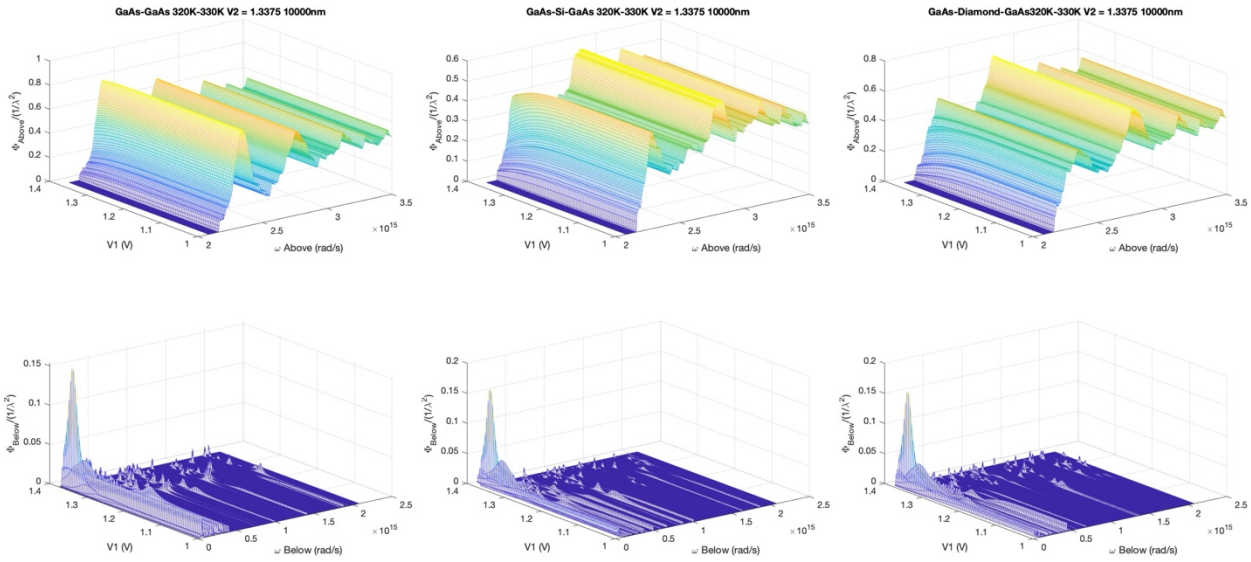

Figure 26. Photon transmission functions for every geometry at 10μm

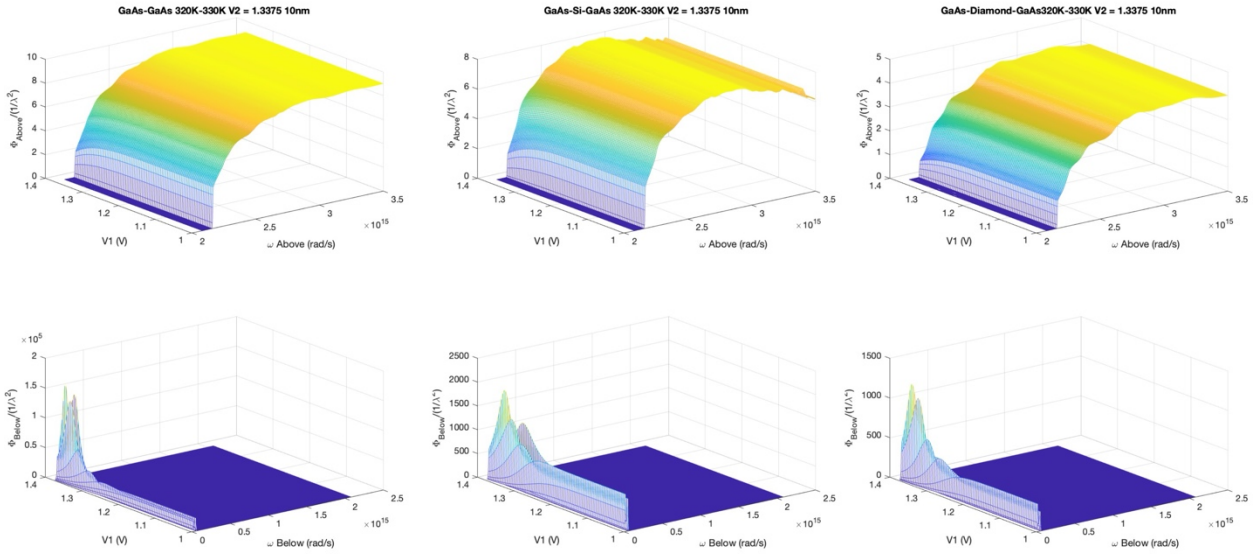

Figure 27. Photon transmission functions for every geometry at 0.01μm

The general trend across all configurations show that as V_2 increases, the functional voltage range of the cooling curve decreases. Since Fig. 11-25 is plotted on a logarithmic scale, the range outside of the curve is when the cooler is producing heat. The optimal COP can be found at a different V_1 for every V_2 in each geometry. By increasing the voltage range for the cooler to exhibit cooling, we are able to choose from a larger set of voltages for an optimal coefficient of performance. To compare the effectiveness between the near-field and far-field cooler, we plot the COP as a function of cooling power. Most of the studies performed showed that the near-field cooler with a high cooling power is inefficient. The near-field cooler is unable to produce the high coefficient of performance for the configurations with no film and an Si film. However, Figs. 23-25 shows that with a diamond film applied when $V_2 > 1.2812$, the near-field cooler begins to show the same high coefficient of performance even with greater cooling power. We also note that diamond can be fabricated using chemical vapor deposition [12].

Chapter 5

Future Improvements

5.1 Limitations

In this thesis, the GaAs LED is simplified by using a thin active layer. In actual device, GaAs LED typically has double hetero-junction structure, used to suppress the surface recombination velocity. We expect that our current model provides similar results to model including cladding layers.

In actual GaAs LED, the metal substrate is not perfect electric conductor, thus directly absorb luminescence of the LED, leading to parasitic heating. When including actual metal layer, photonic structure such as low-index spacer layer or Bragg distributed reflector may be introduced to suppress the absorption of luminescence in the substrate.

5.2 Future improvements

We discuss a few areas that can be explored further. The voltage V_2 could have been assessed at smaller increments to obtain an optimal V_2 for every voltage bias V_1 in every geometry. If an optimal V_2 is obtained, the coefficient of performance can be optimized for every geometry, so that a more complete curve can be obtained. However, the computation time with an extensive list of V_2 values will increase drastically.

Another figure of merit for cooling is the maximum temperature difference between the hot and cold sides to examine the versatility of the cooler. At a bigger temperature difference, the

cooler may not exhibit cooling at all. The temperature drop can be further optimized by using photonic designs.

Chapter 6

Conclusion

This study showed that achieving high cooling power and high coefficient of performance in a near-field electroluminescent cooler is possible by judiciously chosen IR-lossless large bandgap coating material. The use of a diamond film is to reduce parasitic heating in sub-bandgap frequencies for an increase in the coefficient of performance without sacrificing cooling power. Although the goal of this thesis is achieved, many further improvements can be made. As of right now, V_2 has not been optimized for each geometry, so the optimal coefficient of performance has yet to be achieved. The versatility of such a cooler can be investigated by testing larger temperature differences to find a point where it fails to produce any cooling.

The implementation of a solid-state cooler could be very promising, as it is an efficient and high-power solution in a small footprint. Electroluminescent cooling has great potential for achieving efficient and compact cooling for electronics, personal thermal management, domestic, industrial, and space applications.

Appendix A

MATLAB Code for Setup with Diamond Film

A.1 P_template

```
SI;

T1_list = 320;      % temperature of light emitting diode
T2      =330;               % temperature of photodiode

V1_list = 1+0.00375*(0:100);
V2_list = 1+0.00375*[10 50 75 80 90];



%% thickness_parameter

thickness_GaAs_LED  =0.5;
thickness_GaAs_PD    =0.5;
thickness_Si=0.25;
Gap_list=[0.01 10]; % micrometers

% perform the
% computation
for index_V1 = 1:length(V1_list)
```

```
    V1 = V1_list(index_V1);
    for index_V2 = 1:length(V2_list)
        V2 = V2_list(index_V2);

        tic

        for index_Gap=1:length(Gap_list)
            Gap=Gap_list(index_Gap);
            for index_T1=1:length(T1_list)
                T1=T1_list(index_T1);


filename=['./SourceData/',num2str(T1),'/AboveEg_Gap_',num2str(Gap*1e3),'nm_LE
DPD_T_',num2str(T1),'_',num2str(T2),'_V_',num2str(V1),'_',num2str(V2),'.mat']
;
                if ~exist(filename,'file')
                    calcPhi_AboveEg(Gap, thickness_GaAs_LED, thickness_Si,
thickness_GaAs_PD, T1, T2, V1, V2);
                end


filename=['./SourceData/',num2str(T1),'/BelowEg_Gap_',num2str(Gap*1e3),'nm_LE
DPD_T_',num2str(T1),'_',num2str(T2),'_V_',num2str(V1),'_',num2str(V2),'.mat']
;
                if ~exist(filename,'file')
                    calcPhi_BelowEg(Gap, thickness_GaAs_LED, thickness_Si,
thickness_GaAs_PD, T1, T2, V1, V2);
```

```
                end


filename=['./SourceData/',num2str(T1),'/BelowEg_Gap_',num2str(Gap*1e3),'nm_LE
DPD_T_',num2str(T1),'_',num2str(T2),'_V_',num2str(V1),'_',num2str(V2),'.mat']
;
                if ~exist(filename,'file')
                    calcPhi_PV_AboveEg(Gap, thickness_GaAs_LED, thickness_Si,
thickness_GaAs_PD, T1, T2, V1, V2);
                end
            end
        end

        PROCESSING_TIME = toc;
        disp(['V1 = ',num2str(V1),'V2 = ',num2str(V2),'time =
',num2str(PROCESSING_TIME)])

    end
end


disp('done')
```

A.2 calcPhi_PV_AboveEg.m

```
function [wmega_list,phi_list]=calcPhi_PV_AboveEg(GapValue,
thickness_GaAs_LED, thickness_diamond, thickness_GaAs_PD, T1, T2, V1, V2)
% T1 and T2 are temperatures for LED and PD, respectively
% V1 and V2 are voltages for LED and PD, respectively
%% goal: transfer between the whole LED and the whole PD
%% basic parameters

SI;
tic;
eps_vacuum= 1-1j*1e-10;

%% frequency




wmega_list= 2.08e15:0.25e13:3.5e15; % Upper Boundary arbitrarily determined
lambda_um = 2*pi*lightv./(wmega_list*1e-6);
wmega     =wmega_list/lightv/1e6; % 2*pi/lambda_um

%% geometry
% the vacuum gap size in unit of micron
Gap            =GapValue;

doping_GaAs_ND=2e17;
```

```
%% kx setting
kx_list      = [0:0.02:3.98 4*2.^(0:0.1:8)];
kx_step_list = ([kx_list(2)-
kx_list(1),diff(kx_list)]+[diff(kx_list),kx_list(end)-kx_list(end-1)])/2;

%% thickness assignment
thickness_list=[...
    Inf;...
    thickness_GaAs_LED;...
    Gap;...
    thickness_diamond;...
    thickness_GaAs_PD;...
    Inf];

K=3;

%% epsilon eiwt convention
IsLossy           =false(size(thickness_list));
IsLossy((K+2):end)=true;

eps_PEC            = -1e10-1j*1e10;
eps_GaAs_LED       =calceps_DopedGaAs_blocking(lambda_um, doping_GaAs_ND, 0,
T1, V1); % for below bandgap part, do not consider the voltage dependence
eps_GaAs_PD        =calceps_DopedGaAs_blocking(lambda_um, doping_GaAs_ND, 0,
T2, V2); % for below bandgap part, do not consider the voltage dependence
eps_diamond             =calceps_diamond(lambda_um);
```

```
spec    =zeros(length(wmega),length(kx_list));
for index_wmega=1:length(wmega)
    wmega_tmp=wmega(index_wmega);
    eps_list_tmp=[...
        eps_PEC;...
        eps_GaAs_LED(index_wmega);...
        eps_vacuum;...
        eps_diamond(index_wmega);...
        eps_GaAs_PD(index_wmega);...
        eps_PEC];...

    for index_kx=1:length(kx_list)
        kx_tmp=kx_list(index_kx);
        Absorption=calcEmit(wmega_tmp, eps_list_tmp, thickness_list, IsLossy,
kx_tmp, K);
        spec(index_wmega, index_kx)=Absorption.*kx_tmp; % disregard the
vacuum, as here the vacuum is at different T
    end
end
phi_list=sum(spec*diag(kx_step_list),2);

%% finish
t=toc;
title_name=['PV_AboveEg_Gap_',num2str(Gap*1e3),'nm_LEDPD_T_',num2str(T1),'_',
num2str(T2),'_V_',num2str(V1),'_',num2str(V2)];
save([title_name,'.mat'],...
```

```
    'phi_list','lambda_um','wmega_list','t',...
    'thickness_GaAs_LED', 'thickness_GaAs_PD',
'thickness_diamond','T1','T2','V1','V2');
end
```

A.3 calcPhi_BelowEg.m

```
function [wmega_list,phi_list]=calcPhi_BelowEg(GapValue, thickness_GaAs_LED,
thickness_diamond, thickness_GaAs_PD, T1, T2, V1, V2)
% T1 and T2 are temperatures for LED and PD, respectively
% V1 and V2 are voltages for LED and PD, respectively

%% basic parameters

SI;
tic;
eps_vacuum= 1-1j*1e-10;

%% frequency
% wavenumber=[100:2:500, 510:10:1000, 1050:30:7200];



wmega_list= 1e13:0.5e13:2.08e15; % Lower Boundary arbitrarily determined
lambda_um = 2*pi*lightv./(wmega_list*1e-6);
```

```
wmega     =wmega_list/lightv/1e6; % 2*pi/lambda_um

%% geometry
% the vacuum gap size in unit of micron
Gap           =GapValue;

doping_GaAs_ND =2e17;

%% kx setting
kx_list      = [0:0.02:3.98 4*2.^(0:0.1:8)];
kx_step_list = ([kx_list(2)-
kx_list(1),diff(kx_list)]+[diff(kx_list),kx_list(end)-kx_list(end-1)])/2;

%% thickness assignment
thickness_list=[...
    Inf;...
    thickness_GaAs_LED;...
    Gap;...
    thickness_diamond;...
    thickness_GaAs_PD;...
    Inf];

K=3;

%% epsilon eiwt convention
IsLossy           =false(size(thickness_list));
IsLossy((K+1):end)=true;
```

```
eps_PEC            = -1e10-1j*1e10;
eps_GaAs_LED       =calceps_DopedGaAs_blocking(lambda_um, doping_GaAs_ND, 0,
T1, V1); % for below bandgap part, do not consider the voltage dependence
eps_GaAs_PD        =calceps_DopedGaAs_blocking(lambda_um, doping_GaAs_ND, 0,
T2, V2); % for below bandgap part, do not consider the voltage dependence
eps_diamond             =calceps_diamond(lambda_um);

spec    =zeros(length(wmega),length(kx_list));
for index_wmega=1:length(wmega)
    wmega_tmp=wmega(index_wmega);
    eps_list_tmp=[...
        eps_PEC;...
        eps_GaAs_LED(index_wmega);...
        eps_vacuum;...
        eps_diamond(index_wmega);...
        eps_GaAs_PD(index_wmega);...
        eps_PEC];...

    for index_kx=1:length(kx_list)
        kx_tmp=kx_list(index_kx);
        Absorption=calcEmit(wmega_tmp, eps_list_tmp, thickness_list, IsLossy,
kx_tmp, K);
        spec(index_wmega, index_kx)=Absorption.*kx_tmp; % disregard the
vacuum, as here the vacuum is at different T
    end
end
```

```
phi_list=sum(spec*diag(kx_step_list),2);


%% finish
t=toc;
title_name=['BelowEg_Gap_',num2str(Gap*1e3),'nm_LEDPD_T_',num2str(T1),'_',num
2str(T2),'_V_',num2str(V1),'_',num2str(V2)];
save([title_name,'.mat'],...
    'phi_list','lambda_um','wmega_list','t',...
    'thickness_GaAs_LED', 'thickness_GaAs_PD',
'thickness_diamond','T1','T2','V1','V2');
end
```

A.4 calcPhi_AboveEg.m

```
function [wmega_list,phi_list]=calcPhi_AboveEg(GapValue, thickness_GaAs_LED,
thickness_diamond, thickness_GaAs_PD, T1, T2, V1, V2)
% T1 and T2 are temperatures for LED and PD, respectively
% V1 and V2 are voltages for LED and PD, respectively
%% goal: transfer between the whole LED and the whole PD
%% basic parameters

SI;
tic;
eps_vacuum= 1-1j*1e-10;
```

```
%% frequency



wmega_list= 2.08e15:0.25e13:3.5e15; % Upper Boundary arbitrarily determined
lambda_um = 2*pi*lightv./(wmega_list*1e-6);
wmega     =wmega_list/lightv/1e6; % 2*pi/lambda_um

%% geometry
% the vacuum gap size in unit of micron
Gap            =GapValue;

doping_GaAs_ND=2e17;

%% kx setting
kx_list      = [0:0.02:3.98 4*2.^(0:0.1:8)];
kx_step_list = ([kx_list(2)-
kx_list(1),diff(kx_list)]+[diff(kx_list),kx_list(end)-kx_list(end-1)])/2;

%% thickness assignment
thickness_list=[...
    Inf;...
    thickness_GaAs_LED;...
    Gap;...
    thickness_diamond;...
    thickness_GaAs_PD;...
```

```
    Inf];

K=3;

%% epsilon eiwt convention
IsLossy           =false(size(thickness_list));
IsLossy((K+1):end)=true;

eps_PEC            = -1e10-1j*1e10;
eps_GaAs_LED       =calceps_DopedGaAs_blocking(lambda_um, doping_GaAs_ND, 0,
T1, V1); % for below bandgap part, do not consider the voltage dependence
eps_GaAs_PD        =calceps_DopedGaAs_blocking(lambda_um, doping_GaAs_ND, 0,
T2, V2); % for below bandgap part, do not consider the voltage dependence
eps_diamond             =calceps_diamond(lambda_um);

spec    =zeros(length(wmega),length(kx_list));
for index_wmega=1:length(wmega)
    wmega_tmp=wmega(index_wmega);
    eps_list_tmp=[...
        eps_PEC;...
        eps_GaAs_LED(index_wmega);...
        eps_vacuum;...
        eps_diamond(index_wmega);...
        eps_GaAs_PD(index_wmega);...
        eps_PEC];...

    for index_kx=1:length(kx_list)
```

```
        kx_tmp=kx_list(index_kx);
        Absorption=calcEmit(wmega_tmp, eps_list_tmp, thickness_list, IsLossy,
kx_tmp, K);
        spec(index_wmega, index_kx)=Absorption.*kx_tmp; % disregard the
vacuum, as here the vacuum is at different T
    end
end
phi_list=sum(spec*diag(kx_step_list),2);

%% finish
t=toc;
title_name=['AboveEg_Gap_',num2str(Gap*1e3),'nm_LEDPD_T_',num2str(T1),'_',num
2str(T2),'_V_',num2str(V1),'_',num2str(V2)];
save([title_name,'.mat'],...
    'phi_list','lambda_um','wmega_list','t',...
    'thickness_GaAs_LED', 'thickness_GaAs_PD',
'thickness_diamond','T1','T2','V1','V2');
end
```

A.5 calceps_DopedGaAs_blocking.m

```
function eps_list=calceps_DopedGaAs_blocking(lambda, ND, NA, T, V)
% ND, NA in cm^{-3}
% lambda in micron
% V is voltage bias
```

```
% T is temperature in K
SI;

file_name='GaAs_lambda_n_k.dat';

FID=fopen(file_name,'r');
M  =textscan(FID,'%f %f %f','HeaderLines',0);
fclose(FID);
lambda_template=M{1};
n_template=M{2};
k_template=M{3};

eps_r_template=n_template.^2-k_template.^2;
eps_i_template=2*n_template.*k_template;

% bandgap in eV
calc_EG=@(T_template) 1.519-5.405e-4*T_template^2/(T_template+204);
EG     =calc_EG(T); % in unit of eV
EG_300K=calc_EG(300);
dEG    =EG-EG_300K;

% shift the reference spectrum that is above the bandgap of 300 K
feV_template          =2*pi*lightv*hbar./(lambda_template*1e-6)/eV;

index_aboveEg_template               =feV_template>EG_300K;
feV_template(index_aboveEg_template)
=feV_template(index_aboveEg_template)+dEG;
```

```
% for below bandgap, but shorter than 2 micrometers (0.62 eV), remove
% band-edge absorption
index_middle_template                =(feV_template<=EG_300K) &
(feV_template>0.62);
eps_i_template(index_middle_template)=1e-8;

% add a point
feV_template_aboveEg  =feV_template(index_aboveEg_template);
eps_r_template_aboveEg=eps_r_template(index_aboveEg_template);
eps_i_template_aboveEg=eps_i_template(index_aboveEg_template);

feV_template      =[...
    feV_template_aboveEg;...
    feV_template_aboveEg(end)-1e-8;...
    feV_template(~index_aboveEg_template)];
eps_r_template    =[...
    eps_r_template_aboveEg;...
    eps_r_template_aboveEg(end);...
    eps_r_template(~index_aboveEg_template)];
eps_i_template    =[...
    eps_i_template_aboveEg;...
    1e-8;...
    eps_i_template(~index_aboveEg_template)];

lambda_template       =2*pi*lightv*hbar./(feV_template*eV)/1e-6;
```

```
eps_list              =zeros(size(lambda));

%% aboveEg
%% solve quasi-Fermi levels, using ND, NA, T, V
% assume mn and mp independent of temperature
mn     =0.068*me; % effective mass for electrons in condution band
mp     =0.53 *me; % effective mass for holes in valence band

% cover -6*kB*T to the other side
E_step   =1e-3; % in eV
EF_p_list=-(6*kB*T/eV):E_step:3;     % set Ev as zero, p from high to low
EF_n_list=EF_p_list+V-EG;            % w.r.t. Ec, n from low to high

E_c_list =  (0:E_step:3);            % in eV, w.r.t. Ec
E_v_list = -E_c_list;                % in eV, w.r.t. Ev

[EF_n_mg, E_c_mg]=meshgrid(EF_n_list, E_c_list);
[EF_p_mg, E_v_mg]=meshgrid(EF_p_list, E_v_list);

n_mg=mn*sqrt(2*mn)/(pi^2*hbar^3) * sqrt(    E_c_mg *eV ) ./( exp(  (E_c_mg-
EF_n_mg)*eV/(kB*T) ) + 1 );
p_mg=mp*sqrt(2*mp)/(pi^2*hbar^3) * sqrt( (0-E_v_mg)*eV ) ./( exp( -(E_v_mg-
EF_p_mg)*eV/(kB*T) ) + 1 );

n_list=sum(n_mg*(E_step*eV), 1); % in m^{-3}, generated by GaAs
p_list=sum(p_mg*(E_step*eV), 1); % in m^{-3}, generated by GaAs
```

```
n_minus_p_list=n_list-p_list;
EF_p          =interp1(n_minus_p_list, EF_p_list, (ND-NA)*1e6,'linear'); % n
+ (A-)=p + (D+), n and p need states in GaAs
EF_n          =EF_p+V-EG;                                                 %
this is with respect to the EC

n_value=interp1(EF_n_list, n_list, EF_n, 'linear'); % in m^{-3}, only due to
GaAs
p_value=interp1(EF_p_list, p_list, EF_p, 'linear'); % in m^{-3}, only due to
GaAs

%% when V=0, no doping
NC    =2*(2*pi*mn*kB*T/(2*pi*hbar)^2)^1.5;
NV    =2*(2*pi*mp*kB*T/(2*pi*hbar)^2)^1.5;
EF_0  =EG/2+kB*T/(2*eV)*log(NV/NC); % with respect to EV
EF_0_p=EF_0;
EF_0_n=EF_0-EG;

%% compute the nv-nc for each wavelength, only for the range above Eg
wmega_SI      =2*pi*lightv./(lambda*1e-6);
feV           =hbar*wmega_SI/eV;
index_aboveEg =feV>EG;
lambda_aboveEg=lambda(index_aboveEg);
feV_aboveEg   =feV(index_aboveEg);
nc_m_nv_list  =zeros(size(feV_aboveEg));
nc_m_nv_0_list=zeros(size(feV_aboveEg));
for index=1:length(feV_aboveEg)
```

```
    feV_tmp =feV_aboveEg(index);
    E_c_list=( 0:1e-3:1 )   *(feV_tmp-EG);  % feV_tmp>EG required for direct
transition, w.r.t Ec, in eV
    E_v_list=( (-1):1e-3:0 )*(feV_tmp-EG);  % match E_c_list for direct
transition element-wise
    % apply the real units
    nc_m_nv_list(index)=  sum( ...
        ( mn*sqrt(2*mn)/(pi^2*hbar^3)*sqrt( E_c_list*eV) ).*...
        ( mp*sqrt(2*mp)/(pi^2*hbar^3)*sqrt(-E_v_list*eV) ).*...
        ( 1./( exp( (E_v_list-EF_p  )*eV/(kB*T) )+1 ) - 1./( exp( (E_c_list-
EF_n)  *eV/(kB*T) )+1 ) )*...
        (1e-3*(feV_tmp-EG)*eV) );
    nc_m_nv_0_list(index)=sum( ...
        ( mn*sqrt(2*mn)/(pi^2*hbar^3)*sqrt( E_c_list*eV) ).*...
        ( mp*sqrt(2*mp)/(pi^2*hbar^3)*sqrt(-E_v_list*eV) ).*...
        ( 1./( exp( (E_v_list-EF_0_p)*eV/(kB*T) )+1 ) - 1./( exp( (E_c_list-
EF_0_n)*eV/(kB*T) )+1 ) )*...
        (1e-3*(feV_tmp-EG)*eV) );
end
ratio_nc_m_nv=nc_m_nv_list./nc_m_nv_0_list;

%% for above bandgap part, only account for the change in imaginary part due
to Pauli blocking
eps_r_list_aboveEg=interp1(lambda_template,eps_r_template,lambda_aboveEg,'lin
ear');
eps_i_list_aboveEg=interp1(lambda_template,eps_i_template,lambda_aboveEg,'lin
ear');
```

```
eps_i_list_aboveEg     =eps_i_list_aboveEg.*ratio_nc_m_nv; %
eps_list(index_aboveEg)=eps_r_list_aboveEg-1j*eps_i_list_aboveEg;

%% for below bandgap part, account for the free carrier absorption due to
doping and V
lambda_belowEg=lambda(~index_aboveEg);
wmega_belowEg =2*pi*lightv./(lambda_belowEg*1e-6);

% intrinsic, due to phonon, interband etc.
eps_r_list_belowEg=interp1(lambda_template,eps_r_template,lambda_belowEg,'lin
ear');
eps_i_list_belowEg=interp1(lambda_template,eps_i_template,lambda_belowEg,'lin
ear');

% mobility of electron, from Ioffe; the temperature scaling is fitted from
Ioffe
mobility_n=9400/( 1+(ND/1e17)^0.5 )*(T/300)^(-0.7932)*1e-
4;                      % in m^2/(V s)
mobility_p=( 0.0025*(T/300)^2.3 + 4e-21*(p_value/1e6)*(T/300)^1.5 )^(-1) *
1e-4; % in m^2/(V s)

gamma_n   =eV/mn/mobility_n;
gamma_p   =eV/mp/mobility_p;

eps_Drude =...
    -n_value*eV^2/(eps0*mn)./(wmega_belowEg.^2-1j*wmega_belowEg*gamma_n)...
```

```
    -p_value*eV^2/(eps0*mp)./(wmega_belowEg.^2-1j*wmega_belowEg*gamma_p);


eps_list(~index_aboveEg)=(eps_r_list_belowEg-
1j*eps_i_list_belowEg)+eps_Drude;
end
```

A.6 calceps_diamond.m

```
function eps=calceps_diamond(lambda)
% lambda in micron
file_name='diamond_lambda_n_k.dat';

FID=fopen(file_name,'r');
M=textscan(FID,'%f %f %f','HeaderLines',0);
fclose(FID);
lambda_template=M{1};
n_template=M{2};
k_template=M{3};

n_temp=interp1(lambda_template,n_template,lambda);
k_temp=interp1(lambda_template,k_template,lambda);
eps=(n_temp-1j*k_temp).^2;

end
```

A.7 plot_phi.m

```
clear
clf;
SI;

%% parameters

T1      =320;
T2      =330;               % temperature of photodiode

V1_list = 1+0.00375*(0:100);
V2_list = 1+.00375*([10 50 75 80 90]);



Gap_list     =[0.01 10]; % micrometers
Climit  = T1/(T2-T1);

for index_V2=1:length(V2_list)
    clf
    V2=V2_list(index_V2);

    for index_Gap = 1:length(Gap_list)
        Gap=Gap_list(index_Gap);
```

```
        %% Extract data



        filename=['../SourceData/',num2str(T1), '/',
num2str(V2),'/AboveEg_Gap_',num2str(Gap*1e3),'nm_LEDPD_T_',num2str(T1),'_',nu
m2str(T2),'_V_',num2str(V1_list(1)),'_',num2str(V2(1)),'.mat'];
        load(filename,'wmega_list');
        wmega_Above               =wmega_list;
        wmega_step_PV_Above_orig     = diff(wmega_Above);
        wmega_step_PV_Above          =abs( [wmega_step_PV_Above_orig,
wmega_step_PV_Above_orig(end)] + [wmega_step_PV_Above_orig(1),
wmega_step_PV_Above_orig] )/2;
        % ^dealing with size issues, diff() removes element from list
        store_phi_PV_Above           =
zeros(length(V1_list),length(wmega_Above)).*wmega_step_PV_Above;


        filename=['../SourceData/',num2str(T1), '/',
num2str(V2),'/BelowEg_Gap_',num2str(Gap*1e3),'nm_LEDPD_T_',num2str(T1),'_',nu
m2str(T2),'_V_',num2str(V1_list(1)),'_',num2str(V2(1)),'.mat'];
        load(filename,'wmega_list');
        wmega_Below               =wmega_list;
        wmega_step_Below_orig     = diff(wmega_Below);
```

```
        wmega_step_Below          =abs( [wmega_step_Below_orig,
wmega_step_Below_orig(end)] + [wmega_step_Below_orig(1),
wmega_step_Below_orig] )/2;
        store_phi_Below           =
zeros(length(V1_list),length(wmega_Below)).*wmega_step_Below;

        for index_V1=1:length(V1_list)
            V1=V1_list(index_V1);

            filename=['../SourceData/',num2str(T1), '/', num2str(V2),
'/AboveEg_Gap_',num2str(Gap*1e3),'nm_LEDPD_T_',num2str(T1),'_',num2str(T2),'_
V_',num2str(V1),'_',num2str(V2),'.mat'];
            load(filename,'phi_list');

store_phi_PV_Above(index_V1,:)=(wmega_Above/(2*pi*lightv)).^2.*phi_list';

            filename=['../SourceData/',num2str(T1), '/', num2str(V2),
'/BelowEg_Gap_',num2str(Gap*1e3),'nm_LEDPD_T_',num2str(T1),'_',num2str(T2),'_
V_',num2str(V1),'_',num2str(V2),'.mat'];
            load(filename,'phi_list');

store_phi_Below(index_V1,:)=(wmega_Below/(2*pi*lightv)).^2.*phi_list';

        end

        subplot(2,1,1)
        mesh(wmega_Above,V1_list,store_phi_PV_Above);
```

```
        xlabel('wmega Above  ')
        ylabel('V1 (V)')
        zlabel('phi Above')
        title(['GaAs-Diamond-GaAs',num2str(T1),'K-',num2str(T2),'K ', 'V2 =
', num2str(V2), ' ', num2str(Gap*1000), 'nm'])

        subplot(2,1,2)
        mesh(wmega_Below,V1_list,store_phi_Below);
        xlabel('wmega Below  ')
        ylabel('V1 (V)')
        zlabel('phi Below')


        saveas(gcf,[num2str(V2),'V ',num2str(T1),'K ',num2str(Gap*1000),'nm
mesh.png'])

    end
end
```

A.8 main.m

```
clear
clf;
SI;
```

```
%% parameters

T1      =320;
T2      =330;               % temperature of photodiode

V1_list = 1+0.00375*(0:100);
V2_list = 1+0.00375*([10 50 75 80 90]);
% V2_list(end+1) = 0;



Gap_list     =[0.01 10]; % micrometers
Climit  = T1/(T2-T1);


filename=['../SourceData/',num2str(T1), '/',
num2str(V2_list(1)),'/AboveEg_Gap_',num2str(Gap_list(1)*1e3),'nm_LEDPD_T_',nu
m2str(T1),'_',num2str(T2),'_V_',num2str(V1_list(1)),'_',num2str(V2_list(1)),'
.mat'];
load(filename,'wmega_list');
wmega_Above               =wmega_list;
store_plot_phi_Above      =
zeros(length(V1_list),length(wmega_Above),length(Gap_list));
store_phi_Above           =
zeros(length(V1_list),length(wmega_Above),length(Gap_list));
store_wmega_Above         = zeros(length(Gap_list),length(wmega_Above));
```

```
filename=['../SourceData/',num2str(T1), '/',
num2str(V2_list(1)),'/BelowEg_Gap_',num2str(Gap_list(1)*1e3),'nm_LEDPD_T_',nu
m2str(T1),'_',num2str(T2),'_V_',num2str(V1_list(1)),'_',num2str(V2_list(1)),'
.mat'];
load(filename,'wmega_list');
wmega_Below               =wmega_list;
store_plot_phi_Below      =
zeros(length(V1_list),length(wmega_Below),length(Gap_list));
store_phi_Below           =
zeros(length(V1_list),length(wmega_Below),length(Gap_list));
store_wmega_Below         = zeros(length(Gap_list),length(wmega_Below));

filename=['../SourceData/',num2str(T1), '/',
num2str(V2_list(1)),'/PV_AboveEg_Gap_',num2str(Gap_list(1)*1e3),'nm_LEDPD_T_'
,num2str(T1),'_',num2str(T2),'_V_',num2str(V1_list(1)),'_',num2str(V2_list(1)
),'.mat'];
load(filename,'wmega_list');
wmega_PV_Above               =wmega_list;
store_plot_phi_PV_Above      =
zeros(length(V1_list),length(wmega_PV_Above),length(Gap_list));
store_phi_PV_Above           =
zeros(length(V1_list),length(wmega_PV_Above),length(Gap_list));
store_wmega_PV_Above         =
zeros(length(Gap_list),length(wmega_PV_Above));

store_Qc        = zeros(length(Gap_list),length(V1_list));
```

```
store_COP       = zeros(length(Gap_list),length(V1_list));
store_IV        = zeros(length(Gap_list),length(V1_list));
store_F         = zeros(length(Gap_list),length(V1_list));
store_E         = zeros(length(Gap_list),length(V1_list));

for index_V2=1:length(V2_list)
    clf
    V2=V2_list(index_V2);



    for index_Gap = 1:length(Gap_list)
        Gap=Gap_list(index_Gap);
        % thickness_parameter
        thickness_LED=0.5;  in micrometers
        thickness_PV =0.5;
        %% Finding R1
        % Values from Chen JAP 2017
        C1  = 7e-30; % cm^6/s
        C1  = C1*1e-12; % m^6/s converting to SI

        Cn1 = C1/2;  % m^6/s
        Cp1 = C1/2;  % m^6/s

        ni1 = 2.8e5; % cm^-3
        ni1 = ni1*1e6;% m^-3 converting to SI

        tau1= 16.7e-6; %s
```

```
        t1  = thickness_LED*1e-6; %m
        A1  = 1/tau1; %1/s
        NA1 = sqrt(A1/Cp1); % m^-3
        ND1 = 0;
        p1   =0.5*((NA1-ND1)+sqrt((NA1-
ND1)^2+(4*ni1^2*exp(eV*V1_list/(2*kB*T1)))));
        n1   =0.5*((ND1-NA1)+sqrt((ND1-
NA1)^2+(4*ni1^2*exp(eV*V1_list/(2*kB*T1)))));



        % n and p, for LED 1

        R1 = (Cn1*n1 + Cp1*p1).*(n1.*p1 - ni1^2)*t1 + A1*t1*(n1.*p1-
ni1^2)/(n1+p1+2*ni1);

        %% Finding R2
        C2  = 7e-30; % cm^6/s
        C2  = C2*1e-12; % m^6/s converting to SI

        Cn2 = C2/2;  % m^6/s
        Cp2 = C2/2;  % m^6/s

        ni2 = 2.8e5; % cm^-3
        ni2 = ni2*1e6;% m^-3 converting to SI

        tau2= 16.7e-6; % s
```

```
        t2  = thickness_PV*1e-6; % m
        A2  = 1/tau2; % 1/s
        NA2 = sqrt(A2/Cp2); % m^-3
        ND2 = 0;
        p2   =0.5*((NA2-ND2)+sqrt((NA2-
ND2)^2+(4*ni2^2*exp(eV*V2_list/(2*kB*T2)))));
        n2   =0.5*((ND2-NA2)+sqrt((ND2-
NA2)^2+(4*ni2^2*exp(eV*V2_list/(2*kB*T2)))));



        % n and p, for LED 1

        R2 = (Cn2*n2 + Cp2*p2).*(n2.*p2 - ni2^2)*t2 + A2*t2*(n2.*p2-
ni2^2)/(n2+p2+2*ni2);


        %% Extract data



        for index_V1=1:length(V1_list)
            V1=V1_list(index_V1);

            filename=['../SourceData/',num2str(T1), '/', num2str(V2),
'/AboveEg_Gap_',num2str(Gap*1e3),'nm_LEDPD_T_',num2str(T1),'_',num2str(T2),'_
V_',num2str(V1),'_',num2str(V2),'.mat'];
```

```
            load(filename,'phi_list');
            load(filename,'wmega_list')
            store_wmega_Above(index_Gap,:)             = wmega_list;
            store_plot_phi_Above(index_V1,:,index_Gap) = phi_list;

store_phi_Above(index_V1,:,index_Gap)=(store_wmega_Above(index_Gap,:)/(2*pi*l
ightv)).^2.*phi_list';

            filename=['../SourceData/',num2str(T1), '/', num2str(V2),
'/BelowEg_Gap_',num2str(Gap*1e3),'nm_LEDPD_T_',num2str(T1),'_',num2str(T2),'_
V_',num2str(V1),'_',num2str(V2),'.mat'];
            load(filename,'phi_list');
            load(filename,'wmega_list')
            store_plot_phi_Below(index_V1,:,index_Gap) = phi_list;
            store_wmega_Below(index_Gap,:)             = wmega_list;

store_phi_Below(index_V1,:,index_Gap)=(store_wmega_Below(index_Gap,:)/(2*pi*l
ightv)).^2.*phi_list';

            filename=['../SourceData/',num2str(T1), '/', num2str(V2),
'/PV_AboveEg_Gap_',num2str(Gap*1e3),'nm_LEDPD_T_',num2str(T1),'_',num2str(T2)
,'_V_',num2str(V1),'_',num2str(V2),'.mat'];
            load(filename,'phi_list');
            load(filename,'wmega_list')
            store_plot_phi_PV_Above(index_V1,:,index_Gap) = phi_list;
            store_wmega_PV_Above(index_Gap,:)             = wmega_list;
```

```
store_phi_PV_Above(index_V1,:,index_Gap)=(store_wmega_PV_Above(index_Gap,:)/(
2*pi*lightv)).^2.*phi_list';

        end

        %% Calculation

        wmega_step_Above_orig     = diff(store_wmega_Above(index_Gap,:));
        wmega_step_Above          =abs( [wmega_step_Above_orig,
wmega_step_Above_orig(end)] + [wmega_step_Above_orig(1),
wmega_step_Above_orig] )/2;
        % ^dealing with size issues, diff() removes element from list
        wmega_step_Below_orig     = diff(store_wmega_Below(index_Gap,:));
        wmega_step_Below          =abs( [wmega_step_Below_orig,
wmega_step_Below_orig(end)] + [wmega_step_Below_orig(1),
wmega_step_Below_orig] )/2;

        wmega_step_PV_Above_orig     =
diff(store_wmega_PV_Above(index_Gap,:));
        wmega_step_PV_Above          =abs( [wmega_step_PV_Above_orig,
wmega_step_PV_Above_orig(end)] + [wmega_step_PV_Above_orig(1),
wmega_step_PV_Above_orig] )/2;


        for index_V1=1:length(V1_list)
            V1=V1_list(index_V1);
```

```
            Ee = sum(((theta(store_wmega_Above(index_Gap,:),T1,V1)-
theta(store_wmega_Above(index_Gap,:),T2,V2)).*store_phi_Above(index_V1,:,inde
x_Gap)).*wmega_step_Above);

            Ep = sum(((theta(store_wmega_Below(index_Gap,:),T2,0)-
theta(store_wmega_Below(index_Gap,:),T1,0)).*store_phi_Below(index_V1,:,index
_Gap)).*wmega_step_Below);

            F1 =
sum((theta(store_wmega_Above(index_Gap,:),T1,V1)./(hbar*store_wmega_Above(ind
ex_Gap,:)).*store_phi_Above(index_V1,:,index_Gap)).*wmega_step_Above) -...

sum((theta(store_wmega_Above(index_Gap,:),T2,V2)./(hbar*store_wmega_Above(ind
ex_Gap,:)).*store_phi_Above(index_V1,:,index_Gap)).*wmega_step_Above);

            F2 =
sum((theta(store_wmega_PV_Above(index_Gap,:),T1,V1)./(hbar*store_wmega_PV_Abo
ve(index_Gap,:)).*store_phi_PV_Above(index_V1,:,index_Gap)).*wmega_step_PV_Ab
ove) -...

sum((theta(store_wmega_PV_Above(index_Gap,:),T2,V2)./(hbar*store_wmega_PV_Abo
ve(index_Gap,:)).*store_phi_PV_Above(index_V1,:,index_Gap)).*wmega_step_PV_Ab
ove);
```

```
        I1 = eV*(F1+R1(index_V1));
        I2 = ev*(-F2+R2(index_V2));

        Qc               = (Ee-Ep) - I1*V1;
        store_Qc(index_Gap,index_V1)  = Qc;
        store_COP(index_Gap,index_V1) = Qc/(I1*V1+I2*V2);
        store_COP(find(store_Qc < 0)) = NaN;
        % store_F(index_Gap,index_V1) = F;
        store_E(index_Gap,index_V1) = Ee-Ep;



    end



end

%% V1 plot
store_COP = store_COP/Climit;

subplot(3,1,1)
semilogy(V1_list,store_Qc)
ylabel('Qc (W/m^2)')
xlim([0.99 1.385])
ylim([1e-2 1e6])
```

```
    title(['GaAs-Diamond',num2str(T1),'K-',num2str(T2),'K ', 'V2 = ',
num2str(V2)])



    subplot(3,1,2)
    plot(V1_list,store_COP)
    xlabel('V1 (V)')
    ylabel('COP/Carnot')
    xlim([0.99 1.385])
    ylim([0 1])
    legend(num2str(Gap_list(1)), num2str(Gap_list(2)))

    subplot(3,1,3)
    semilogx(store_Qc(1,:),store_COP(1,:))
    hold on
    semilogx(store_Qc(2,:),store_COP(2,:))
    xlabel('Qc (W/m^2)')
    ylabel('COP/Carnot')
    xlim([1e-2 1e6])
    ylim([0 1])

    if V2 ==0
        saveas(gcf,['no recovery ',num2str(T1),'K
',num2str(Gap_list*1000),'nm.png'])
    else
```

```
        saveas(gcf,['recovery ', num2str(V2),'V ',num2str(T1),'K
',num2str(Gap_list*1000),'nm.png'])
    end


end


%% Theta plot
% V1_list = linspace(1,1.375,length(wmega_Above));
% store_Theta = zeros(length(V1_list),length(wmega_Above));
%
% for index_V1 = 1:length(V1_list)
%     V1 = V1_list(index_V1);
%     Theta = theta(wmega_Above,T1,V1);
%     store_Theta(index_V1,:) = Theta;
% end
% plot = store_Theta./(hbar*wmega_Above);
% mesh(V1_list,wmega_Above,plot)
```

A.9 SI.m

```
lightv=2.99792458e8;
hbar  =1.054571726e-34;
```

```
kB    =1.3806488e-23;
kb    =kB;
mu0   =4*pi*1e-7;
eps0  =8.854187817e-12;
eV    =1.602176565e-19;
ev    =eV;
me =9.10938291e-31;

fontsize=20;
linewidth=1;
```

A.10 theta.m

```
function APE = theta(wmega,T,V)
% Bose-Einstein Distribution
    SI
    APE = (hbar*wmega)./(exp((hbar*wmega-eV*V)/(kB*T))-1);

end
```

Bibliography

[1] T. L. Bergman and Adrienne. Lavine, *Fundamentals of heat and mass transfer.*, 8th ed. Hoboken, NJ: John Wiley & Sons, Inc., 2017.

[2] Polder D. and Van Hove M., "Theory of Radiative Heat Transfer between Closely Spaced Bodies," *Phys Rev B*, vol. 48, no. 10, Nov. 1971, doi: https://doi.org/10.1103/PhysRevB.4.3303.

[3] G. C. Dousmanis, C. W. Mveller, H. Nelson, and K. G. Petzinger, "Evidence of Refrigerating Action by Means of Photon Emission in Semiconductor Diodes "N recent studies of recombination radiation in GaAs," *Physical Review*, vol. 113, no. 1A, pp. A316–A318, 1964, doi: https://doi.org/10.1103/PhysRev.133.A316.

[4] T. Sadi, I. Radevici, and J. Oksanen, "Thermophotonic cooling with light-emitting diodes," *Nature Photonics*, vol. 14, no. 4. Nature Research, pp. 205–214, Apr. 01, 2020. doi: 10.1038/s41566-020-0600-6.

[5] H. Gauck, T. H. Gfroerer, M. J. Renn, E. A. Cornell, and K. A. Bertness, "External radiative quantum efficiency of 96% from a GaAs /GaInP heterostructure," 1997. doi: https://doi.org/10.1007/s003390050455.

[6] P. Santhanam, D. J. Gray, and R. J. Ram, "Thermoelectrically pumped light-emitting diodes operating above unity efficiency," *Phys Rev Lett*, vol. 108, no. 9, pp. A316–A318, Feb. 2012, doi: 10.1103/PhysRevLett.108.097403.

[7] K. Chen, P. Santhanam, S. Sandhu, L. Zhu, and S. Fan, "Heat-flux control and solid-state cooling by regulating chemical potential of photons in near-field electromagnetic heat transfer," *Phys Rev B Condens Matter Mater Phys*, vol. 91, no. 13, Apr. 2015, doi: 10.1103/PhysRevB.91.134301.

[8] P. Wurfel, "The chemical potential of radiation," *J. Phys. C: Solid State Phys*, vol. 15, pp. 3967–3985, 1982, doi: 10.1088/0022-3719/15/18/012.

[9] B. Song, A. Fiorino, E. Meyhofer, and P. Reddy, "Near-field radiative thermal transport: From theory to experiment," *AIP Adv*, vol. 5, no. 5, May 2015, doi: 10.1063/1.4919048.

[10] K. Chen, T. P. Xiao, P. Santhanam, E. Yablonovitch, and S. Fan, "High-performance near-field electroluminescent refrigeration device consisting of a GaAs light emitting diode and a Si photovoltaic cell," *J Appl Phys*, vol. 122, no. 14, Oct. 2017, doi: 10.1063/1.5007712.

[11] T. Patrick Xiao, K. Chen, P. Santhanam, S. Fan, and E. Yablonovitch, "Electroluminescent refrigeration by ultra-efficient GaAs light-emitting diodes," *J Appl Phys*, vol. 123, no. 17, May 2018, doi: 10.1063/1.5019764.

[12] M. Jiang *et al.*, "Diamond formation mechanism in chemical vapor deposition," *PNAS*, vol. 119, no. 16, 2022, doi: 10.1073/pnas.2201451119.